University of the Basque Country

UPV EHU

www.mscnano.eu

Master's in Nanoscience

MASTER THESIS

"Electron Cooling in Nanoscale Superconducting Structures"

by

Mikel Rouco

Supervisor(s): F. Sebastian Bergeret

Date of defense: 13 July 2017

Acknowledgements

This master thesis would not exist as it is without the help and support from a lot of people.

Fist of all, I would like to express my deep gratitude to F. Sebastian Bergeret for the direction of this Master's Thesis and for his permanent attention in my work. I appreciate his suggestions, support and involvement in the project, which helped me throughout the whole process. I also want to thank his affability and the good treatment that I experienced from the beginning.

I am also grateful to Tero Heikkilä for the very meaningful information and the always (good) ideas that he gave us during the process.

I have to thank Maitane for her patience and the encouragement, even at the worst moments of this process, and for trying to help me at all times.

I am obliged to Ane for the selfless final revision and correction of the text, especially considering her lack or time.

I would like to thank my family and friends for their unconditional support and for making posible see the light.

My thanks to the people who share office and group with me, that in some occasion help me doing my work.

Finally, I shall not forget my class and group colleagues. Thanks for the sometimes necessary, but always pleasant, good moments and distractions.

Contents

Chapter 1

Introduction.

Since superconductivity was discovered by H. Kamerlingh Onnes (Leiden) in 1911 [1], it has been used for wide range of practical purposes. Among all the applications, the most notable ones rely on their use as zero-resistance elements to produce strong magnetic fields (*e.g.* Large Hadron Collider at CERN), as ideal diamagnets to levitate objects (*e.g.* Japan Maglev trains) and as precision detectors, either to measure currents [2, 3] or magnetic fields with SQUIDs [4] (Superconducting QUantum Interference Device).

Conventional superconductors with low T_c are very useful in the fabrication of structures with sizes smaller than the characteristic coherence length (typically micron-size). In recent decades, the great achievement in making high-quality contacts between superconductors, normal metals, ferromagnets and insulators has allowed the controlled building of nanostructures small enough to show quantum phenomena.

New technologies focused on miniaturization of electronic solid-state circuits face significant obstacles. Decreasing the size and increasing the speed of transistors, leads to large ohmic dissipation and the associated heating. For that reason, there is an increasing interest in the study of heat management and control at the nanoscale. The branch of electronics that studies the coupling between the charge and heat currents is known as *caloritronics*. If one adds the spin degree of freedom, one talks about *spin caloritronics*.

In properly biased hybrid nanostructures, the superconducting gap can be used as an energy filter that cools down the adjacent material by selectively allowing high-energy "hot" quasiparticles to tunnel to the superconductor. The flow of charge current in normal metal - insulator - superconductor (N-I-S) tunnel junctions at a bias voltage V is accompanied by a heat transfer from N into S. That heat transfer through N-I-S junctions can be used for the realization of microcoolers [5, 6, 7]. We extend these studies by considering the use of spin filters in the junction and Zeeman fields in the superconductor with the aim of increasing the cooling power.

In the present work, we explore the field of spin caloritronics by using supercon-

ductors, normal metals, insulators and ferromagnetic insulators as building blocks. To that end, in chapter 3 we first introduce the formalism used and present some basic usage examples of it. In chapter 4 we present the concept of cooling power and study it in a N-I-S structure. Replacing the insulating layer by a spin-splitting one, we also reproduce some recent results [8] that suggest the enhancement of cooling power in these configurations.

Finally, we devote chapter 5 to discuss some novel results obtained over the course of this Master's Thesis. We study how superconductors with a spin-split density of states can be used to improve the cooling power and refrigeration at the nanoscale. The spin-splitting can be achieved by an external magnetic field or by the proximity of an adjacent ferromagnetic insulator. We show that on the one hand, the spin-splitting opens the possibility of refrigerating the superconducting electrode. This is not usually possible and, in addition to its fundamental interest it might even be useful for some quantum applications. On the other hand, we demonstrate that the maximum cooling power in a normal metal in contact with a spin-split superconductor, is achieved at lower values of the bias voltage V. This implies lower ohmic dissipation rates. As a result, the refrigeration of the metallic sample is enhanced by a neighbouring spin-split superconductor when the volume of the latter is comparable to that of the former. The results of this Master's Thesis are being discussed in an article which is in process [9].

Chapter 2

Landauer-Büttiker Formalism.

In this chapter we review the Landauer-Büttiker formalism that is suitable for the description of electronic transport in mesoscopic structures. This formalism will be generalized in subsequent chapters for cases in which superconductivity is present in the system. The formalism presented in this chapter was introduced for the first time by Landauer [10, 11] for systems with only two terminals. Afterwards, Büttiker *et al.* (among which Landauer was) extended it for more general cases [12].

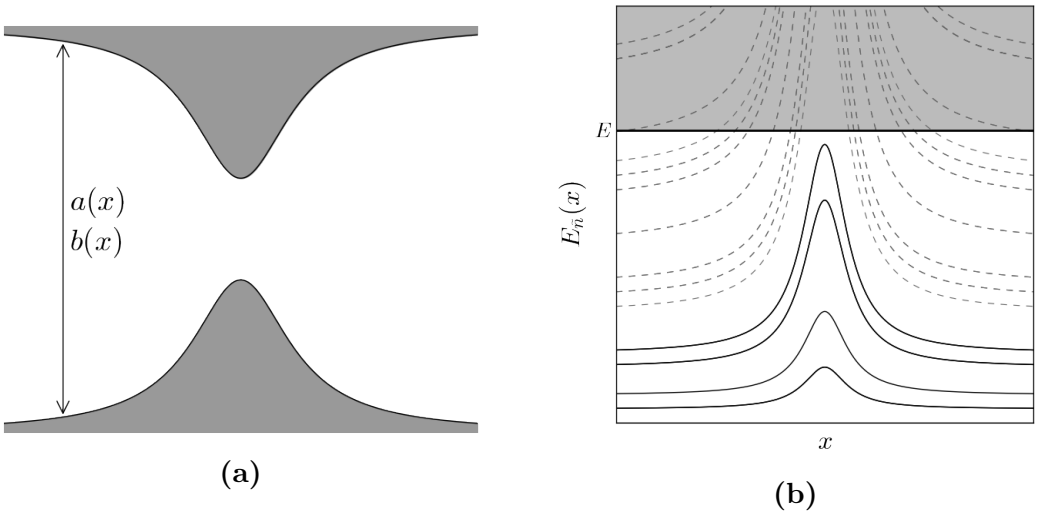

Figure 2.1: ***(a)*** *Cross section of a rectangular adiabatic QPC (either along y or z direction) and* ***(b)*** *the effective potential energy due to the constriction. At a given energy, E, only the transport levels (solid lines) are open.*

The Landauer-Büttiker formalism describes the transport through a ballistic region attached to well-defined electrodes with zero resistances. For example, the intermediate region can be, for example, a *quantum point contact* (QPC), which was first studied by van Wees et al. in 1988 [13]. By means of their experimental study, the verification of a big amount of previous theoretical works was enabled. They consist in a narrow constriction between the two electrodes, with a width similar to the electron wavelength. Therefore, this constriction will be translated into a confinement, causing some appreciable quantum effects.

The behaviour of electronic transport in a QPC can be studied as a free electron gas traveling through a rectangular *waveguide* with a variable cross section that confines it. In Fig. 2.1a the cross section of the structure along the direction of propagation is represented in a schematic way. If the size of the cross section varies over distances much larger than the electronic wavelength, we can calculate the confinement energy of the electron in each point along the propagation direction, x, as an infinite rectangular potential of dimensions $a(x) \times b(x)$. The results of this calculations are reflected in Fig. 2.1b, where the constriction in the quantum point contanct behaving as a potential barrier can be seen.

This barrier has a direct consequence of great importance: not every electron living in one of the electrodes will be able to travel through the structure. From a conventional view, only those particles whose energy is greater than the one of the potential barrier would be transmitted. However, this barrier depends on the confinement state level n, which are the quantum numbers of the rectangular potential well that describes the *transversal component* of the electronic wavefunction). In the quantum transport jargon, these are known as *transmission channels*. In Fig. 2.1b solid lines represent *open conduction channels* for a carrier of energy E, i.e. possible rectangular potential eigenfunctions describing the electronic wavefunction perpendicular to the x axis whose eigenvalues (the energy) are always lower than E. Therefore, depending on carrier's energy, more or less transmission channels will be *open* modifying electronic properties in the nanostructure; specially its electric conductance.

Taking into account that the velocity of propagation of a particle along the direction x is given by $\hbar v_x = \partial E/\partial k_x$, one can derive the current flowing along a structure like the one in Fig. 2.1 biased with a potential V. To achieve that, one writes the electric current through the contact as the normalized sum over the whole momentum space of the multiplication of the velocity of the electron times its probability of jumping from one electrode to the other one, i.e:

$$I = 2_s e \sum_{\mathrm{n}} \int_{-\infty}^{\infty} \frac{dk_x}{2\pi} v_x(k_x) \Big[f_L(k_x) - f_R(k_x) \Big] = \frac{2_s e}{2\pi\hbar} \sum_{\mathrm{n:open}} \int dE \Big[f_L(E) - f_R(E) \Big] =$$
$$= \frac{2_s e}{h} N_{\mathrm{open}} (\mu_L - \mu_R) = G_0 N_{\mathrm{open}} V. \tag{2.1}$$

In these equations the notation 2_s is used for the factor coming from spin degeneracy, $\mu \equiv \mu_L - \mu_r = eV$ and $G_0 \equiv \frac{2e^2}{h} \approx 7.75 \times 10^{-5}\ S$ is the quantum of the conductance. This result suggests that electric conductance is quantized, which was experimentally verified in 1988 by the same Dutch group that first reported a QPC [13] as well as by some others [14]. This derivation assumes a pure ballistic case, i.e. when no impurities are present in the sample. The effect of scattering centers can be included by assuming a finite transmission, $0 \leq \mathcal{T}_n \leq 1$, for each of the channels. Thus, the complete Landauer formula [10, 11] reads:

$$I = \left[\sum_{\mathrm{n}} \mathcal{T}_n(\mu) G_0 \right] V. \tag{2.2}$$

This simple expression is a powerful tool to describe the electronic transport in a mesoscopic region attached to electrodes, being all the information about the structure stored in the transmission coefficients, $\mathcal{T}_n$. In the case of normal (non-superconducting) nanostructures Eq. 2.2 describes most of the transport features. This is applied when the quasiparticles of the structure behaves as the real particles, i.e. electrons. In the superconducting case, however, it is not the case.

Superconductors are macroscopically coherent quantum systems with a characteristic electronic structure that distinguishes them from normal metals, insulators or semiconductors. Regarding quantum transport, the opening of a gap, $\Delta \sim meV$, in which Cooper's pairs lives, is of great importance. This coherent condensate is the origin of several effects, such as the Josephson effect or Andreev reflections. Moreover, quasiparticles are a linear combination of electrons and holes.

These sort of effects, in which the phase coherence plays a crucial role, cannot be described by Eq. 2.2. Thus, in the following chapter we will generalize the formalism that this equation describes for the case in which superconducting correlations are present.

Chapter 3

Semiclassical Transport. Introduction and Basic Examples.

In the previous chapter we have reviewed the Landauer-Büttiker quantum transport formalism and discussed its limitations. At first glance, one could think about using a full scattering-matrix formulation of any transport problem in order to go beyond the Landauer-Büttiker approach. This would work for idealised structures without any defect or impurity. However, in realistic systems, each impurity acts as a scattering center, re-emitting incoming waves that have to be included in the wave function, and turning the true quantum picture hopelessly complicated.

One can find a solution by renouncing to a full microscopic description and adopting a semiclassical picture [15]. In such case, one describes electrons as a statistical ensemble of quasiparticles characterized by their (space-time) coordinates, x, and (quasi)momenta, p, by means of a function. This approach can be justified taking into account that for quasiparticles in a metal $\delta p \approx \hbar k_F$ and substituting it in Heisenberg uncertainty relation, $\delta x \delta p \geq \hbar/2$. Therefore, the classical limit is reached when the function characterizing the ensamble slowly depends on the space-time coordinates (in particular when $\delta r \gg k_F^{-1}$, where k_F is the wavenumber of quasiparticles at the Fermi surface).

However, a purely classical approach to transport, such as one based on Boltzmann or drift-diffusion equation, would disregard the coherence of electron waves from the very begining, and thus, it is not useful for a description of quantum transport. We need therefore a semiclassical rigurous formalism that preserves, at least partially, this coherence. Such formalism is based on the *semiclassical Green's functions*.

In the present work we are not going to present the derivation of the semiclassical Green's functions' formalism. We refer those readers interested in details to the book by Zagoskin [16]. In the next section we will introduce the Green's functions, set the notation that we will use throughout the work and solve some basic training problems.

3.1 Basic Concepts

In this section we introduce the basic tools that are being used in subsequent chapters. From now on, we set $\hbar = 1$ and $k_B = 1$ unless we explicitly write them.

3.1.1 One-particle Green's Functions

Green's functions are a powerful quantum field theoretical tool in many body problems. In this section we outline how they can be obtained, within the quasiclassical approximation, to describe mesoscopic normal metal and superconducting systems. We refer readers interested in details to the book in Ref. [16].

First, we write the Green's function in Nambu space, which combine the particle and hole space. Using pseudo-spinors as a compact notation, $\hat{\Psi}^\dagger = (\Psi_\uparrow^\dagger, \Psi_\downarrow)$, we can express the time ordered GF as:

$$\hat{\mathcal{G}} = -i \left\langle T\ \hat{\Psi}(x_1)\hat{\Psi}^\dagger(x_1')\right\rangle = \begin{pmatrix} \mathcal{G}(x_1, x_1') & \mathcal{F}(x_1, x_1') \\ \mathcal{F}^\dagger(x_1, x_1') & \mathcal{G}^\dagger(x_1, x_1') \end{pmatrix}, \tag{3.1}$$

where x_1 and x_1' represent sets of space and time coordinates. The Green's function present an *anomalous* component, the pair amplitude $\mathcal{F} = -i\left\langle T\Psi_\uparrow\Psi_\downarrow\right\rangle$, so characteristic for superconducting systems. These functions satisfy Gor'kov equation of motion [17],

$$(\hat{\mathcal{G}}_0^{-1} - \hat{\Delta} - \hat{\Sigma}_{\text{imp}})(x_1, x_2) * \hat{\mathcal{G}}(x_2, x_1') = \delta(x_1, x_1'), \tag{3.2}$$

where $*$ includes a convolution over coordinates. These GFs oscilate as a function of the relative coordinate $|\mathbf{r} - \mathbf{r}'|$ on a scale of the Fermi wavelength λ_F. However, this is much shorter than the characteristic lengths in superconducting problems, given by $\xi_0 = v_F/\Delta$ and $\xi_T = v_F/2\pi T$.

In the quasiclassical approximation we ignore the fast oscillations of $\hat{\mathcal{G}}$ as a function of $|\mathbf{r} - \mathbf{r}'|$. Moreover, we have to pay attention to the dependece of the transport direction, i.e. on the direction of the velocity $\mathbf{v}_F$. Writing $\hat{\mathcal{G}}(\xi, \mathbf{v}_F, \mathbf{r}, E)$, where $\xi \equiv \frac{p^2}{2m} - \mu$ depends on the magnitude of the momentum, the quasiclassical Green's functions are obtained:

$$G(\mathbf{r}, \mathbf{v}_F, E) \equiv \frac{i}{\pi} \int d\xi \hat{\mathcal{G}}(\xi, \mathbf{v}_F, \mathbf{r}, E). \tag{3.3}$$

Finally, during this work we will always work in the diffusive (or dirty) limit. The system has so many impurities that, from the point of view of one of its electrons, it is isotropic in every direction. Hence, we average the quasiclassical GFs over all the possible directions of their velocity $\mathbf{v}_F$:

$$G(\mathbf{r}, E) \equiv \int d\Omega G(\mathbf{r}, \mathbf{v}_F, E). \tag{3.4}$$

In this work, we use the quasiclassical Green's functions in Eq. 3.4. In particular, we mainly focus on the case where the system is considered infinite and homogeneous and hence the GFs only depend on the energy.

3.1.2 Spaces and Pauli Matrices

Green's functions have a matricial structure that appears due to its symmetry that is usually described via Pauli matrices in order to simplify future algebraic operations thanks to their conmutation and anticonmutation relations,

$$[\hat{\sigma}_i, \hat{\sigma}_j] = 2i\epsilon_{ijk}\hat{\sigma}_k, \qquad \{\hat{\sigma}_i, \hat{\sigma}_j\} = 2\delta_{ij}. \tag{3.5}$$

In the present work we study superconducting, magnetic, out-of-equilibrium systems. Therefore, the most generic matrix structure for the GF comprises the direct (tensorial) product of three spaces:

- **Keldysh space.** In order to describe non-equilibrium situations we use the Keldysh formalism. This is defined in a two dimensional space in which Green's functions are triangular, with the retarded, G^R, and advanced, G^A, components in the diagonal and a so called *Keldysh component* in the corner, G^K, as follows:
$$\begin{pmatrix} G^R & G^K \\ 0 & G^A \end{pmatrix}.$$
- **Nambu space.** As we know from BCS theory, quasiparticle excitations in a superconductor are described by linear combinations of quasi-electrons and quasi-holes. Thus, for the description of superconducting correlations it is convenient to extend the quasiparticle space to the one of the electron-hole. In this work we describe this two dimensional *Nambu space*, using Pauli matrices labeled by $\hat{\tau}_i$.
- **Spin space.** In situations in which ferromagnetism or external magnetic fields are involved, the spin space must be taken into account. In this space, Pauli matrices will be labeled by $\hat{\sigma}_i$.

3.1.3 Green's Functions

In this section we present the quasiclassical GFs that are used in this work. They can be obtained from the microscopic or Gor'kov Green's functions. We refer those readers interested in this derivation to the reference [16]. Firstly, it should be highlighted that in this section we do not take into account the effect of the magnetic field and, hence, quasiclassical GFs will not present spin structure, such that $\check{G} = \check{G} \otimes \hat{\sigma}_0$. The way in which splitting fields affects to Green's functions is discussed in following chapters.

Green's Function of a Normal Metal

Within the quasiclassical approach the spectrum of a normal metal is trivially flat. This is manifested in the retarded and advanced GFs that, in the *Nambu* (electron-hole) space are written as:

$$\hat{G}^R_N = \hat{\tau}_3, \qquad \hat{G}^A_N = -\hat{\tau}_3. \tag{3.6}$$

Moreover we have the Keldysh component,

$$\hat{G}_N^K = \hat{G}_N^R \hat{F} - \hat{F}\hat{G}_N^A, \tag{3.7}$$

which contains information about the voltage and temperature dependant occupation of the states described by the symmetrized distribution function:

$$\hat{F} = \tfrac{1}{2}\left(\tanh\tfrac{E+eV}{2T} + \tanh\tfrac{E-eV}{2T}\right) + \tfrac{1}{2}\left(\tanh\tfrac{E+eV}{2T} - \tanh\tfrac{E-eV}{2T}\right)\hat{\tau}_3 \equiv F_+ + F_-\hat{\tau}_3. \tag{3.8}$$

The normalized density of states (DOS) is defined via the GFs as follows:

$$\mathcal{N}(E) \equiv \tfrac{1}{2}\mathrm{Tr}\left[\hat{\tau}_3\left(\hat{G}^R - \hat{G}^A\right)\right], \tag{3.9}$$

which in a normal metal equals the unity matrix. Another important identity that can be checked is the relation of normalization of the Green's function, i.e. $\check{G}_N^2 = \check{1}$.

Green's Function of a Superconductor

In conventional superconductors electrons with energies around the Fermi energy form a condensate of pairs, the so called Cooper pairs. The description of these states in terms of Green's functions requires to include two particles correlations, the Gor'kov or anomalous GFs, f. Furthermore, superconductivity is a macroscopic quantum coherent state and, hence, its phase, φ, is a quantity of great importance that explicitly appears on the Green's functions:

$$\begin{aligned}
\hat{G}_S^R &= g^R\hat{\tau}_3 + if^R(\hat{\tau}_2\cos\varphi + \hat{\tau}_1\sin\varphi),\\
\hat{G}_S^A &= g^A\hat{\tau}_3 + if^A(\hat{\tau}_2\cos\varphi + \hat{\tau}_1\sin\varphi),\\
\hat{G}_S^K &= \hat{G}_S^R\hat{F} - \hat{F}\hat{G}_S^A.
\end{aligned} \tag{3.10}$$

In the previous expressions g and f stand for the standard and anomalous Green's functions respectively and equals

$$g^{R/A}(E) = \frac{E \pm i\eta}{\sqrt{(E\pm i\eta)^2 - \Delta^2}}, \tag{3.11}$$

$$f^{R/A}(E) = \frac{\Delta}{\sqrt{(E\pm i\eta)^2 - \Delta^2}}, \tag{3.12}$$

where Δ is the modulus of the superconducting order parameter and η is known as *damping parameter* that, besides moving the poles below or over the real axis, modelizes impurity effects in the superconductor. In these expressions the branch cut of the square root is unconventionaly chosen as the positive real axis (which is rendered in the branch cuts shown in Fig. 3.1a for the roots in the denominators of g and f) such that 3.9 is still fulfilled. The reduced density of states in the superconductor reads:

$$\mathcal{N}_S(E) = \frac{1}{2}\left[g^R(E) - g^A(E)\right]. \tag{3.13}$$

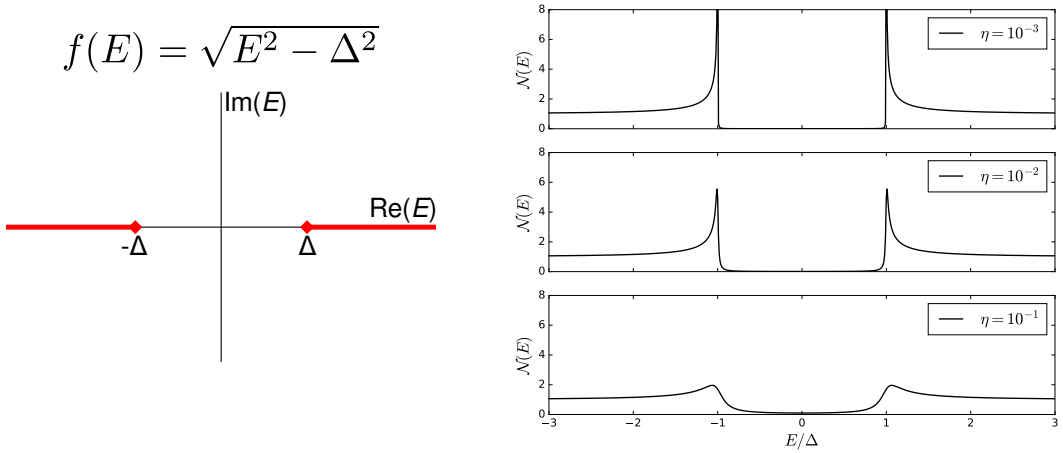

(a) **(b)**

Figure 3.1: ***(a)*** *Branch cuts positions for the square root expression in the denominator of $g(E)$ and $f(E)$.* ***(b)*** *Broadening of the peaks in the reduced density of states of a superconductor when damping parameter, η, is increased.*

Therefore, the density of states depends on the paremeter η. In particular, when this parameter is increased the characteristic peaks that can be seen in the borders of the superconducting gap are lowered and broadened, as shown in: Fig. 3.1b.

It is important to notice that while the standard Green's functions, $g(E)$, reflect the information of the electronic structure of quasiparticles, the anomalous ones, $f(E)$, are the ones that describe the structure of the superconducting condensate. This can be deduced by observing that in the Green's function of a normal metal the Nambu space is diagonal (quasiparticles in the metal are *well-behaved*), whilst these anomalous ones are off-diagonal (in superconductivity, quasiparticles are a linear combination of electrons and holes). Furthermore, we can check that in the limit where $\Delta = 0$ Green's function of normal metals are recovered.

Regarding to the Keldysh component, as the insertion of a voltage in a superconductor leads to time dependant phases (*AC Josephson Effect*) that hamper the algebra, in this work we avoid applying the voltage on the superconductor. Hence, we work with $\hat{F} \equiv \hat{\tau}_0 F_0 = \tanh \frac{E}{2T}$.

3.2 Usadel Equation and Current Matrix Formalism

As we have previously discussed, the drift-diffusion equation disregards the coherence of the superconducting phase from the very beginning. Nevertheless, there is an analogous equation, which is valid at scales exceeding the mean free path, that takes into account those quantum effects. It is known as Usadel equation and reads:

$$iD\nabla\check{\mathbf{j}} - \left[\check{E}, \check{G}\right] = 0; \qquad \check{\mathbf{j}} = \check{G}\nabla\check{G}, \tag{3.14}$$

where D stands for the diffusion constant, $\check{E} \equiv \epsilon\hat{\tau}_3 + \frac{1}{2}\Delta e^{i\varphi}(i\hat{\tau}_2 + \hat{\tau}_1) + \frac{1}{2}\Delta e^{-i\varphi}(i\hat{\tau}_2 - \hat{\tau}_1)$ $\big(+ \ldots \big)$ is the expression of the self energy of the system that varies between normal metals, ferromagnets and superconductors, among others. In addition, the quantity $\check{\mathbf{j}}$ stands for the current matrix that plays an important role in quantum transport, which in bulk systems is expressed by means of the GFs as shown in Eq. 3.14. From this matrix we obtain the different currents of charge, energy and spin by taking proper traces over the $Nambu \times Spin$ space of the Keldysh component.

When instead of bulk properties, the goal is to obtain the current flow through a barrier or scattering region between two electrodes, we have to add some boundary conditions to the Usadel equation. This yields an expression for the current matrix for any two electrodes, known as Nazarov equation [18]:

$$\check{J} = \sum_n 2\tau_n \left[\check{G}_l, \check{G}_R\right] \cdot \left[4 - \tau_n \left(2 - \left\{\check{G}_L, \check{G}_R\right\}\right)\right]^{-1}. \tag{3.15}$$

In this equation the sum is performed over open conduction channels, τ_n is the transmission of each channel, the subscripts are named L and R, which mean $left$ and $right$, and $[\cdot,\cdot]$ and $\{\cdot,\cdot\}$ stand for conmutator and anticonmutator respectively. In the following examples it is ascertained how from the Keldysh component of this matrix, currents of different electronic degrees of freedom can be described. The most relevant currents are:

$$\begin{aligned} I &= \tfrac{e}{8h} \textstyle\int dE\ \mathrm{Tr}[\hat{\tau}_3 \check{J}^K] \quad &- \quad &\text{Charge current} \\ Q &= \tfrac{1}{8h} \textstyle\int dE\ E\ \mathrm{Tr}[\check{J}^K] \quad &- \quad &\text{Energy current} \\ S &= \tfrac{1}{32\pi} \textstyle\int dE\ \mathrm{Tr}[\hat{\sigma}_3 \check{J}^K] \quad &- \quad &\text{Spin current} \end{aligned} \tag{3.16}$$

Each trace of the $Nambu \times spin$ space reflects one current symmetry. For example, while electrons and holes contribute equally to the energy current, they certainly do not do it in the same way to the electric one, as they have opposite charge. That electron/hole or spin up/down contrary contribution to the charge is included multiplying the $\check{J}^K$ matrix by $\hat{\tau}_3$ or $\hat{\sigma}_3$ respectively. Finally, charge current is given in units of e (the electron charge), whereas the spin current is given in units of $\frac{\hbar}{2}$ for the spin of electron-like fermions. The last ones are integrated over the energy to obtain the whole current and divided by h to obtain the correct units.

3.3 Example 1: Ohm's Law

Firstly, to exemplify how to apply Eq. 3.15-3.16 to transport situations we analyze the electronic transport through a metallic structure. Starting from Eq. 3.15, we recover the Ohm's Law of conduction. Obviously, there are much simpler ways to obtain the Ohm's law that do not involve Keldysh GFs. However, this simple example will illustrate how to use the formalism that we apply in the subsequent sections. As this is the first one it will be done step by step.

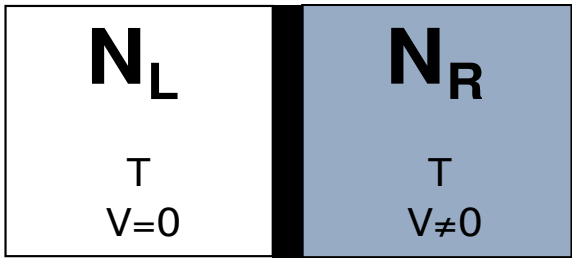

Figure 3.2: *Resistive junction between two metallic infinite electrodes. Both reservoirs are at the same temperature and the voltage is applied on the left.*

We consider a junction composed by two normal metals at the same temperature. A voltage bias, V, is applied across the junction. Per definition, electrodes have a negligible electric resistance and therefore the voltage drop is assumed to happen at the tunneling barrier (see Fig. 3.2). In order to apply the formalism described by Eqs. 3.15-3.16, we write down the GFs of the electrodes, which in the normal case have a simple form:

$$\begin{aligned}
\hat{G}_L^R &= \hat{G}_R^R = \hat{\tau}_3, \\
\hat{G}_L^A &= \hat{G}_R^A = -\hat{\tau}_3, \\
\hat{G}_L^K &= \hat{G}_L^R \hat{F}_L - \hat{F}_L \hat{G}_L^A = 2\hat{\tau}_3 F_0, \\
\hat{G}_R^K &= \hat{G}_R^R \hat{F}_R - \hat{F}_R \hat{G}_R^A = 2\hat{\tau}_3 \left(F_+ + F_- \hat{\tau}_3\right),
\end{aligned}$$

where $F_0 \equiv \tanh \frac{E}{2T}$ and $F_\pm \equiv \frac{1}{2}(\tanh \frac{E+eV}{2T} \pm \tanh \frac{E-eV}{2T})$. The above GFs are used to compute the current matrix in Eq. 3.15. In this case, as the anticonmutator results to be $\{\hat{G}_L, \hat{G}_R\} = 2$, the denominator is the unit matrix multiplied by 4. Introducing the above GFs into Eq. 3.15 we obtain the following Keldysh component of the current matrix:

$$\hat{J}^K(E) = \sum_n 2\tau_n \left(F_+ - F_0 + \hat{\tau}_3 F_-\right).$$

Now, we can substitute this expression in Eq. 3.16 obtaining the next charge current:

$$I = \frac{e}{4h} \int dE \ \mathrm{Tr}\left[\hat{\tau}_3 \hat{J}^K\right] = \frac{e \sum_n \tau_n}{2h} \int dE \left(\tanh \frac{E+eV}{2T} - \tanh \frac{E-eV}{2T}\right) =$$

$$= \sum_n \tau_n \frac{2e^2}{h} V \equiv \sum_n \tau_n G_0 V = G_T V, \tag{3.17}$$

where the factor 2 stems from the trace over spin, $G_0 \equiv \frac{2e^2}{h}$ is the quantum of conductance and $G_T = \sum_n \tau_n G_0$ stands for the total conductance of the contact, or the inverse of the contant resistance. Eq. 3.17 is nothing but the Ohm's law. Notice that the conductance is given by the sum of transmission of the different conducting channels multiplied by the quantum of conductance, according to the

Landauer-Büttiker formalism.

Moreover, it is easy to check that heat and spin currents are zero in the present setup.

3.4 Example 2: Heat Transport and Wiedemann-Franz Law

Now, we study a slightly different case in which we still have two metallic electrodes but instead of being at different electric potential they are temperature biased (Fig. 3.3). This can be experimentally achieved with a dissipative electric current flowing along an electrode placed next to the one that we want to heat up [19] or by putting the electrodes in any temperature bath.

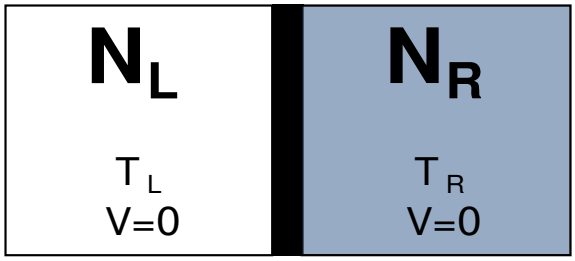

Figure 3.3: *Resistive junction between two metallic infinite electrodes. Both electrodes are at the same potential, but at different temperatures.*

In this situation the Green's functions read:

$$\begin{aligned}
\hat{G}_L^R &= \hat{G}_R^R = \hat{\tau}_3, \\
\hat{G}_L^A &= \hat{G}_R^A = -\hat{\tau}_3, \\
\hat{G}_L^K &= 2\hat{\tau}_3 \tanh \tfrac{E}{2T_L} \equiv 2\hat{\tau}_n F_{0L}, \\
\hat{G}_R^K &= 2\hat{\tau}_3 \tanh \tfrac{E}{2T_R} \equiv 2\hat{\tau}_n F_{0R},
\end{aligned}$$

where the only differences from the previous example lie on the distribution functions. The substitution of these GFs in Eq. 3.15 yields to the following Keldysh component of the current matrix,

$$\hat{J}^K = \sum_n 2\tau_n \left(F_{0R} - F_{0L}\right). \tag{3.18}$$

Finally, we obtain from 3.16 that, whereas the electric current vanishes, the heat or energy current flows through the juntion. The latter is given by

$$Q = \frac{\sum_n \tau_n}{h} \int dE\ E \left(\tanh \frac{E}{2T_R} - \tanh \frac{E}{2T_L} \right) = \sum_n \tau_n \frac{\pi^2}{3h} \left(T_L^2 - T_R^2 \right) =$$

$$= \frac{\pi^2 G_T}{6e^2} \left(T_L^2 - T_R^2 \right), \tag{3.19}$$

where the integral is done by parts and using the equality $\int_{-\infty}^{\infty} dx\ x^2\ \mathrm{sech}^2 x = \frac{\pi^2}{6}$. Recovering the Boltzmann constant multiplying the temperature that has been set to one until now, and assuming a small temperature difference in Eq. 3.19, with $T_R = T$ and $T_L = T + \delta T$, we obtain:

$$Q = \frac{\pi^2 G_T}{3} \left(\frac{k_B}{e} \right)^2 T \delta T \equiv K \delta T, \tag{3.20}$$

where K is the thermal conductance of the junction. As the conductance in the previous example, this quantity depends exclusively on the transmission coefficients, τ_n. Now, the Wiedemann-Franz law can be obtained taking the ratio between the electric and thermal conductance, cf. Eqs. 3.17 and 3.20:

$$\frac{K}{G_T} = \frac{\kappa}{\sigma_T} = \frac{\pi^2}{3} \left(\frac{k_B}{e} \right)^2 T, \tag{3.21}$$

where κ and σ_T are the thermal and electrical conductivity of the system respectively. The proportionality constant, $L \equiv \frac{\pi^2}{3} \frac{k_B}{e}$, is known as the Lorenz number. The realation shown in Eq. 3.21 is valid when $T \to 0$, where the heat and charge currents are mainly carried by quasiparticles. At higher temperatures, two mechanisms produce a deviation of the ratio L: *(i)* other thermal carriers such as phonons and *(ii)* inelastic scattering.

3.5 Example 3: Josephson effect

The previous examples ilustrated how to obtain Landauer-Büttiker equation for the conductances from the more general equation 3.15. Though, the full power of the formalism used in this work can be appreciated considering superconducting element. Here we study a system composed by two phase biased superconducting electrodes, i.e. we assume that there is a phase difference between the two electrodes (Sec. 3.1.3), as shown in Fig. 3.4. We focus on the electrical current that may flow through the junction in abscence of an applied voltage. This is the so called DC Josephson effect that cannot be deduced from the Landauer-Büttiker formalism.

As there is not potential bias between the superconducting electrodes, the difference between their coherence phases will remain constant, so we can set one of the phases to zero. In this case the Green's functions read:

$$\hat{G}_L^{R(A)} = g^{R(A)} \hat{\tau}_3 + i f^{R(A)} \hat{\tau}_2,$$
$$\hat{G}_R^{R(A)} = g^{R(A)} \hat{\tau}_3 + i f^{R(A)} \left(\hat{\tau}_2 \cos\varphi + \hat{\tau}_1 \sin\varphi \right),$$
$$\hat{G}_{L/R}^{K} = \left(\hat{G}_{L/R}^{R} - \hat{G}_{L/R}^{A} \right) F_0,$$

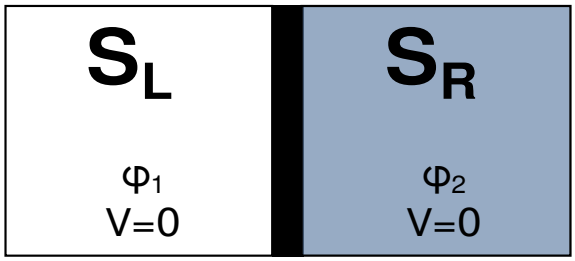

Figure 3.4: *Junction between two superconducting infinite electrodes with different coherence phases. Both electrodes are at the same potential and temperature.*

where $F_0 = \tanh\frac{E}{2T}$ and the expressions of the standard, $g^{R(A)}$, and anomalous, $f^{R(A)}$, GFs were given in Eq. 3.11-3.12. The substitution of these Green's functions into Eq. 3.15 results in a denominator that no longer behaves as a scalar and needs to be inverted. However, the triangular structure of these matrices simplifies their inversion, as from the matricial equation $\check{G}\check{G}^{-1} = 1$ it can be easily shown that

$$\begin{aligned}
\left(\hat{G}^{-1}\right)^R &= \left(\hat{G}^R\right)^{-1}, \\
\left(\hat{G}^{-1}\right)^A &= \left(\hat{G}^A\right)^{-1}, \\
\left(\hat{G}^{-1}\right)^K &= -\left(\hat{G}^{-1}\right)^R \hat{G}^K \left(\hat{G}^{-1}\right)^A.
\end{aligned} \tag{3.22}$$

The final expresion of the current matrix' Keldysh component gets way more complex that in the previous examples. Nevertheless, as we only focus on the charge current, only those components proportional to $\hat{\tau}_3$ in $\hat{J}^K$ contribute (see Eq. 3.16). We obtain the following expression for the spectral current:

$$\begin{aligned}
I(E) &\equiv \frac{e\sum_n \tau_n}{4h}\mathrm{Tr}\left[\hat{\tau}_3\hat{J}^K\right] = \\
&= i\frac{e}{h}\frac{\tanh\frac{E}{2T}\sum_n \tau_n}{2}\left[\frac{(f^R)^2}{1+(f^R)^2\sin^2\frac{\varphi}{2}} - \frac{(f^A)^2}{1+(f^A)^2\sin^2\frac{\varphi}{2}}\right]\sin\varphi = \\
&= i\frac{e}{h}\frac{\Delta^2\sum_n \tau_n}{2}\left[\frac{\tanh\frac{E}{2T}}{(E+i\eta)^2-\Delta^2(1-\Delta^2\sin^2\frac{\varphi}{2})} - \frac{\tanh\frac{E}{2T}}{(E-i\eta)^2-\Delta^2(1-\Delta^2\sin^2\frac{\varphi}{2})}\right]\sin\varphi.
\end{aligned} \tag{3.23}$$

As it can be seen above, electric current in this system depends explicitly on retarded and advanced anomalous Green's functions, which immediatly suggests that its existance is related to the superconducting condensate. In the normal case the anomalous GFs are zero, $f^{R(A)} = 0$, and hence the electric current vanishes, as is expected in a zero voltage situation.

In order to obtain the total current we need to integrate Eq. 3.23 over the energy. This integral can be computed by using the residue theorem. One can see that in Eq. 3.23 we have explicitly split the expression in square brackets in two

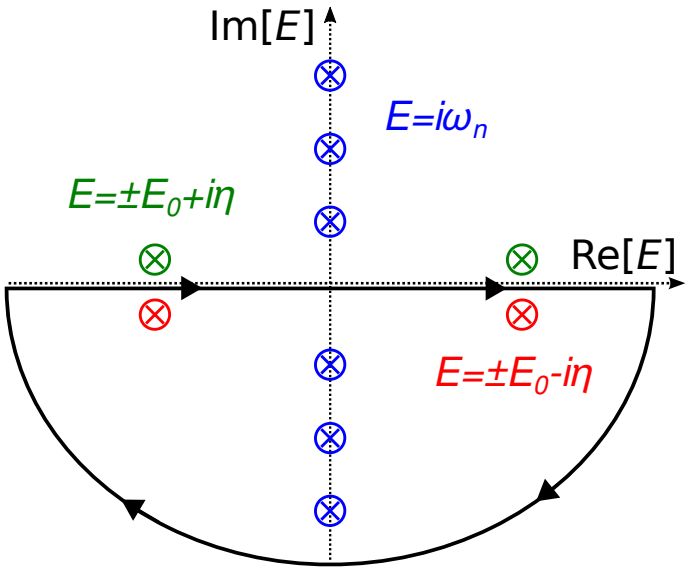

Figure 3.5: *(black) Contour along which the integral has been evaluated and poles that appear (red) only in the "retarded" integrand, (green) only in the advances one or (blue) in both of them.*

summands: one containing the retarded GFs, which will be named as $\mathcal{F}^R(E)$ and depends on $(E+i\eta)$, and the other containing the advanced ones, refered to as $\mathcal{F}^A(E)$.

In these integrands, poles come both from the denominator and from the hyperbolic tangent for the following values of energy:

$$\mathcal{F}^R : \begin{cases} \tanh & \rightarrow \quad E = iT\pi(2m+1) \equiv i\omega_n \\ \text{denominator} & \rightarrow \quad E = \pm\Delta\sqrt{1-\tau_n \sin^2\frac{\varphi}{2}} - i\eta \equiv \pm E_0 - i\eta \end{cases}$$

$$\mathcal{F}^A : \begin{cases} \tanh & \rightarrow \quad E = iT\pi(2m+1) \equiv i\omega_n \\ \text{denominator} & \rightarrow \quad E = \pm\Delta\sqrt{1-\tau_n \sin^2\frac{\varphi}{2}} + i\eta \equiv \pm E_0 + i\eta \end{cases}$$

where ω_n are known as *Matsubara frequencies*. Residue's value at these poles are presented hereunder:

$$\mathcal{F}^R : \begin{cases} \text{Res}\left[\mathcal{F}^R; E = E_0 - i\eta\right] = \text{Res}\left[\mathcal{F}^R; E = -E_0 - i\eta\right] = \frac{\tanh\frac{E_0}{2T}}{2E_0} \\ \text{Res}\left[\mathcal{F}^R; E = i\omega_n\right] = \frac{-2T}{\omega_n^2 + E_0^2} \end{cases}$$

$$\mathcal{F}^A : \begin{cases} \text{Res}\left[\mathcal{F}^A; E = E_0 + i\eta\right] = \text{Res}\left[\mathcal{F}^R; E = -E_0 + i\eta\right] = \frac{\tanh\frac{E_0}{2T}}{2E_0} \\ \text{Res}\left[\mathcal{F}^A; E = i\omega_n\right] = \frac{-2T}{\omega_n^2 + E_0^2} \end{cases}$$

where the $\eta \rightarrow 0$ limit is taken. Thus, the integral over the contour shown in Fig.

3.5, excluding all the constants that do not enter in the integral, is evaluated as follows:

$$\oint_C dE\ I(E) = \int_{-\infty}^{\infty} dE\ I(E) + \int_{\Gamma} dE\ I(E) \propto -2\pi i \frac{\tanh \frac{E_0}{2T}}{E_0}. \tag{3.24}$$

In the expression above the Matsubara poles coming from $\mathcal{F}^R$ are cancelled by the $\mathcal{F}^A$ ones, and only poles coming from the denominator remain. Moreover, as the integrator converges to zero at $E \to \infty$ faster than $\frac{1}{E}$, the integral over the semicircle Γ results in a zero-sum. Consequently, the total supercurrent that flows along the juntion is given by:

$$I = \frac{1}{h} \sum_n \tau_n \pi e \Delta \frac{\tanh \frac{\Delta \sqrt{1 - \tau_n \sin^2 \frac{\varphi}{2}}}{2T}}{\sqrt{1 - \tau_n \sin^2 \frac{\varphi}{2}}} \sin \varphi, \qquad \varphi \in [-\pi, \pi]. \tag{3.25}$$

Usually, the Josephson effect is studied in the tunneling limit and expressed by:

$$I = I_C \sin \varphi, \tag{3.26}$$

where I_C is known as the *critical current* and does not depend on the superconducting phase. However, Eq. 3.25 is valid for any transmission value τ_n and hence, the current-phase relation is different. Taking the $\tau_n \to 0$ limit in Eq. 3.25 and comparing it with Eq. 3.26 we deduce that the critical current is given by:

$$I_C = \frac{1}{h} \sum_n \tau_n \pi e \Delta \tanh \frac{\Delta}{2T}. \tag{3.27}$$

Chapter 4

Electron Cooling in N-S Structures.

Heat currents and dissipation often limit the performance of electronic devices, especially at cryogenic temperatures. In general, cooling a device to lower temperatures increases its sensitivity and decreases noise. Despite the fast progress in cooling techniques without cryogens at the liquid phase, refrigeration to cryogenic temperatures remains expensive and, typically, only feasible in specialized laboratories with the proper infrastructure. Therefore, it is of interest to explore cooling techniques that operate directly on a chip, even though they may be an option just in cases of special applications, that could provide an economic and easy-to-use alternative solution to the final stage of refrigeration.

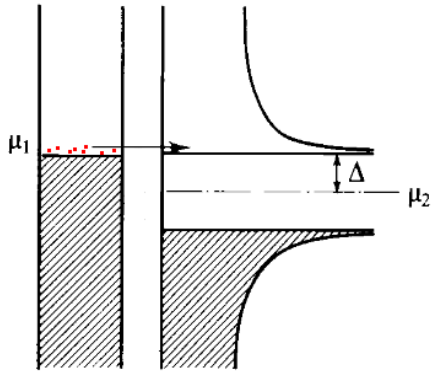

Figure 4.1: *Hot electrons (red) extracted from the normal metal using a superconductor. The superconducting gap acts as an energy filter allowing only high energy electrons to be removed from the metallic electrode.*

In this chapter, we focus on low temperature electronic on-chip coolers based on superconducting hybrid devices. The basic principle of operation is shown in Fig. 4.1. By applying a voltage bias just below the gap energy, the superconducting gap acts as an energy filter that only lets to extract high energy electrons from the metal; leading to cooling of the latter. This concept is also applicable to holes.

This cooling technique was first proposed in the 90's and since then, cooling in normal metal - insulator - superconductor tunneling contacts had been widely theoretically studied [20, 5, 6] and experimentally verified [21, 22, 7], which have reported electronic refrigeration of normal metals from $300mK$ to about $100mK$. Many achievements in this area have been extensively covered and compiled in some reviews [6, 23].

The aim of this chapter is to apply the current matrix formalism introduced in Sec. 3.2 to the study of cooling in junctions between superconducting and metallic electrodes separated by a normal insulating layer (sec. 4.1) or a spin polarizing one (sec. 4.2). In doing so, some new concepts, such as cooling power and electron-phonon coupling are introduced.

4.1 Cooling power in S-I-N junctions

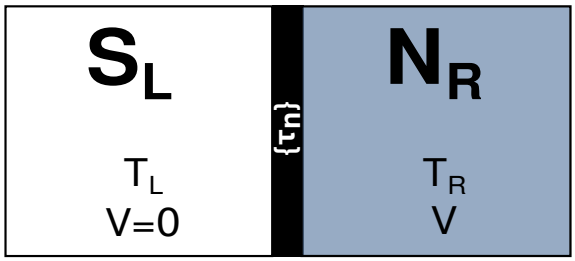

Figure 4.2: *Resistive junction between a metallic and a superconducting electrodes with tuneable transmission. Both reservoirs are at the same temperature but electrostatically biased by a potential V.*

In this section we study the cooling power in a S-I-N structure (Fig. 4.2) in terms of the barrier conductance, which is given as the sum of the transmissions of all the N-S interface's conducting channels, as discussed in Sec. 3.3. In order to apply Eq. 3.15 and calculate the charge and heat currents, we need the Green's functions of the normal ($\check{G}_L$) and superconducting ($\check{G}_R$) electrodes:

$$\begin{aligned}
\hat{G}_L^{R(A)} &= g^{R(A)}\hat{\tau}_3 + if^{R(A)}\hat{\tau}_3, \\
\hat{G}_R^{R} &= -\hat{G}_R^{A} = \hat{\tau}_3, \\
\hat{G}_L^{K} &= \left(\hat{G}_L^{R} - \hat{G}_L^{A}\right) F_0, \\
\hat{G}_R^{K} &= 2\hat{\tau}_3 \left(F_+ + F_-\hat{\tau}_3\right),
\end{aligned}$$

where we set a gauge in which the superconducting phase is zero, such that GFs of the superconductor do not depend on φ, and the algebra is simplified. The substitution of these expressions in Eq. 3.15 yields a rather cumbersome Keldysh component of the current matrix. In order to obtain the charge and heat current we have to multiply this expression by $\hat{\tau}_3$ and $\hat{\tau}_0$ respectively, and take the trace (see Eq. 3.16). Finally we obtain:

$$I = \sum_n \tau_n \frac{e}{h} \int dE \, \frac{\left[-(2-\tau_n(1-g^R))(g^R-g^A)+\tau_n f^R(f^R+f^A)\right] F_-}{(2-\tau_n(1-g^R))(2-\tau_n(1+g^A))}, \tag{4.1}$$

$$Q = \sum_n \frac{\tau_n}{h} \int dE \; E \frac{\left[(2-\tau_n(1-g^R))(g^R-g^A)-\tau_n f^R(f^R-f^A)\right] (F_+-F_0)}{(2-\tau_n(1-g^R))(2-\tau_n(1+g^A))}. \tag{4.2}$$

In the numerator of these equations we can distinguish two contributions to the current. On the one hand, we have terms containing g^R and g^A that describes quasiparticle transport happening at energies out of the superconducting gap, such as $2(g^R - g^A) = 4\mathcal{N}_N\mathcal{N}_S$ and $\tau_n(1-g^R)(g^R-g^A)$. The former equals four times the multiplication of the density of states of the metal and the superconductor, whereas the later is a second order contribution that describes quasiparticle interference effects due to the coherent nature of the superconducting phase. On the other hand, the terms containing anomalous GFs f^R and f^A describe transport efects where the Cooper pairs condensate take part. They can be present for energies inside the superconducting the gap, *i.e. Andreev reflections*, or outside of it. The energies at which each term contribute can be seen in Fig. 4.4.

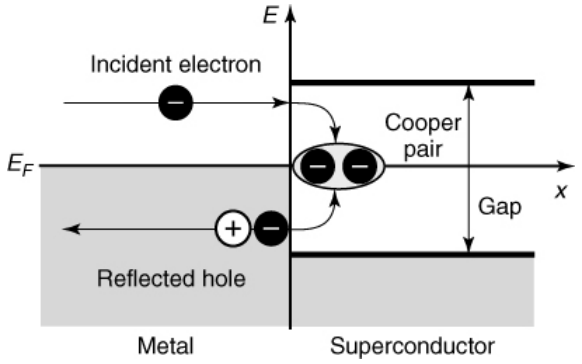

Figure 4.3: *Andreev reflection in a N-S interface. An electron is backscattered as a hole and a Cooper pair is formed in the superconductor.*

Andreev reflections are scattering processes that take place in interfaces between superconductors and metals in which an electron from the metallic electrode is backscattered as a hole, and a Cooper pair is formed in the superconductor. Due to this charge-transfer process, a normal current in the metal is transformed into a supercurrent. This effect is lost when the junction is so resistive that quasiparticles in the metal cannot interact with those in the superconductor; which can be verified with Eqs. 4.1-4.2 in the tunnel limit ($\tau_n \to 0$). It can be easily verified as well that setting $g^{R/A} = \pm 1$ and $f^R = f^A = 0$ (i.e. converting the GFs of the superconductor into those of a normal metal), Eq. 3.17 is obtained.

We analitically solved the integral of the charge current expression (Eq. 4.1) in the tunnel limit and at zero temperature. Applying these conditions and substituting the expressions for the normal GFs, $g^{R/A}$, the charge current through the junction reads:

$$
\begin{aligned}
I &= \sum_n \frac{e\tau_n}{2h} \int dE \left(\frac{E-i\eta}{\sqrt{(E-i\eta)^2-\Delta^2}} - \frac{E+i\eta}{\sqrt{(E+i\eta)^2-\Delta^2}} \right) (\theta(E-eV) - \theta(E-eV)) = \\
&= \sum_n \frac{e\tau_n}{2h} \int dE \left(\sqrt{(E+i\eta)^2-\Delta^2} - \sqrt{(E-i\eta)^2-\Delta^2} \right) (\delta(E+eV) - \delta(E-eV)) = \\
&= \sum_n \frac{e\tau_n}{h} \left(\sqrt{(eV-i\eta)^2-\Delta^2} - \sqrt{(eV+i\eta)^2-\Delta^2} \right) = \\
&= \begin{cases} 0 & |eV| < \Delta \\ -\mathrm{sgn}(eV)\, G_T \sqrt{(eV)^2-\Delta^2}/e & |eV| > \Delta \end{cases} ,
\end{aligned}
\tag{4.3}
$$

where $\theta(x)$ stands for the Heavyside step function and $\mathrm{sgn}(eV)$ is the sign function. In the second step above integration by parts was performed, and in the last one, previously defined branch cuts of the square root are taken into consideration. There is a minus before the sign function in the last expression of Eq. 4.3 because we are applying the voltage in the right electrode, whereas the currents are supposed to be positive when they flow from the left electrode to the right one. In the following, however, we might change the sign to the currents in order to deal with positive values.

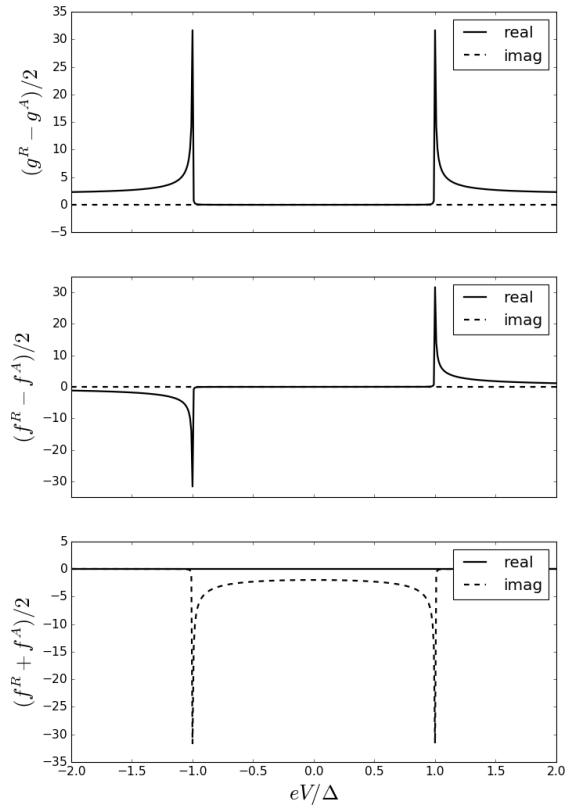

Figure 4.4: *Spectral plots of the real and imaginary parts of the sum and substraction between retarded and advanced superconducting normal and anomalous GFs.*

Beyond the tunneling regime, the currents from Eqs. 4.1-4.2 are calculated numerically. In Fig. 4.5 charge and heat current curves are plotted for a single transport channel with different values of the transmission coefficient, τ_n, and $T_N, T_S \to 0K$. Both currents are normalized to τ_n in order to compare their shapes in one single plot.

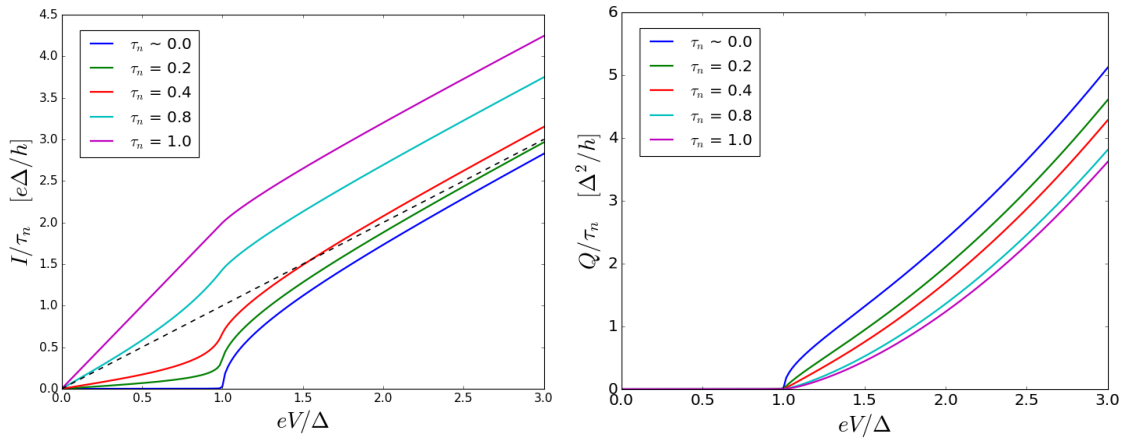

(a) **(b)**

Figure 4.5: *Normalized* ***(a)*** *charge and* ***(b)*** *heat currents in terms of the applied voltage through a single conducting channel with different transission coefficients of a SIN junction, at $T_N, T_S \to 0K$. In* ***(a)*** *dashed line shows the electric current of a NIN junction.*

By increasing the transmission of the contact one increases the probability of the Andreev reflection. This leads to an increase of the subgap current as shown in Fig. 4.5a. From this figure one can see that in perfectly transparent junctions ($\tau_n = 1$) the slope of the $I(V)$ curve, *i.e.* the conductance, for voltages inside the gap doubles the one of a junction between two metals. As mentioned above, decreasing the value of the transmission coefficient turns off Andreev reflections up to the point where there is no electric current inside the gap in the tunnel limit. It is worth noticing that the current for $eV \gg \Delta$ does not coincide with the I-V characteristic of a normal junction (see dashed line in Fig. 4.5a). In particular for finite values of τ the current at large voltages is larger than in the N case. This is the so called excess current, which is defined as the difference between the current at high voltages ($eV \to \infty$) of a SN junction and a junction between two normal metals. The easy measurement of this effect makes it really useful in experimental studies, and it can be observed in Fig. 4.5a, comparing the current curve of the NIS junction for $\tau_n = 1$ with the one of the NIN junction (dashed line) at high applied voltages.

Let us now analyze the heat transport in the junction. Eq. 4.2 describes the rate of energy carried by quasiparticles from the left to the right reservoir. Though, it does not contain all the heating contributions in the system. The bias voltage sets a dissipative current that causes the *Joule heating*. Therefore, we define the cooling

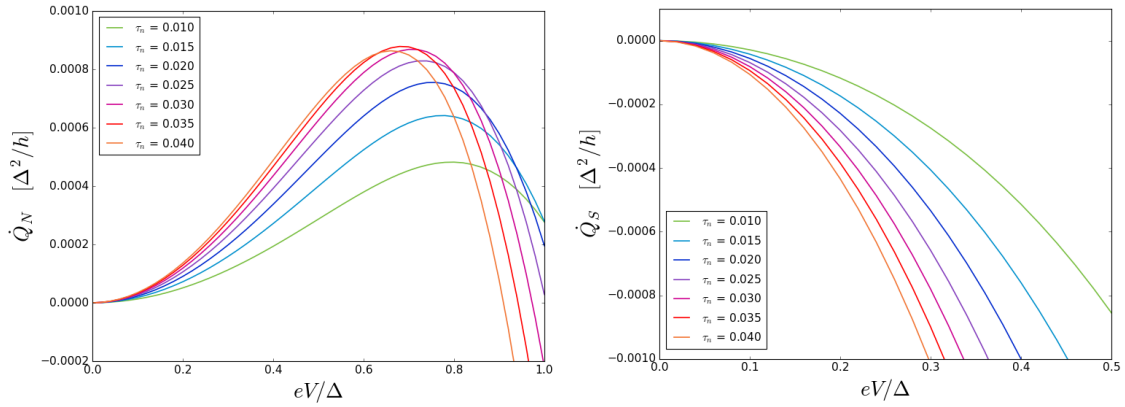

(a) **(b)**

Figure 4.6: *Cooling power in the* ***(a)*** *metallic and* ***(b)*** *superconducting electrodes in terms of the applied voltage and for different values of* τ_n *and* $T_N = T_S = 0.5T_c$*. The metallic electrode can be cooled down, while the superconducting one cannot.*

power in each electrode,

$$\dot{Q}_S = Q, \qquad \dot{Q}_N = -Q + IV, \tag{4.4}$$

as the total ammount of energy flowing out the electrode per unit time. A positive value of $\dot{Q}_j$ means a cooling of the j electrode. In Fig. 4.6 both cooling powers of Eq. 4.4 are plotted for different values of τ_n and $T_N = T_S = 0.5T_C$ ($T_C \approx 1.76\Delta$ is the critical temperature of the superconducting phase), showing that the normal metal present a cooling regime, while the superconducting electrode does not. This was expected from the discussion in the opening of this chapter, where we connected the superconducting gap with an energy filter. We also found the optimum conditions to achieve maximum cooling power in the normal metal,

$$\dot{Q}_N^{\max} = \dot{Q}_N(\tau_n \approx 0.35, T \approx 0.52T_C, eV \approx 0.68\Delta) \approx 0.0009\Delta^2/h \sim 0.1\mu W, \tag{4.5}$$

which, as will be explained, can be improved by substituting the insulating layer by a spin filtering one that turns off Andreev currents.

4.2 Spin-filtering interface. S-sf-N Junction.

As discussed previously, the superconducting gap has been considered an energy filter that allows the electronic cooling of the normal electrode in a properly biased N-S junction (see Fig. 4.1). This image is valid in the tunnel limit, where the conduction is carried out exclusively by quasiparticles. However, when we set higher transparencies of the junction (in order to maximize the cooling power), a second order process, called Andreev current, appears to be a significant transport mechanism. This effect increases the charge current (see Fig. 4.5a), hence increasing the Joule heating term entering Eq. 4.4. This results in a drop of the cooling power. Hence, suppression of Andreev reflections would enhance the cooling in the normal

metal.

Given that Andreev currents involve an electron with spin up (down) and a hole with spin down (up) (both spin polarizations) a spin-filtering device would suppress them. In turn, Joule heating should be overcomed. In this section we study how spin-filter barriers affect the cooling of a normal metal, $\dot{Q}_N$, in a S-sf-N structure. The spin-filter barrier is characterized by its transmission coefficients, $\tau_n \in [0, 1]$, and its efficiency in a given direction, $p \in [-1, 1]$. Ideal candidates for such barriers are som Europium chalcogenides with spin-filter efficiency of almost 100% ($p = 1$) [24].

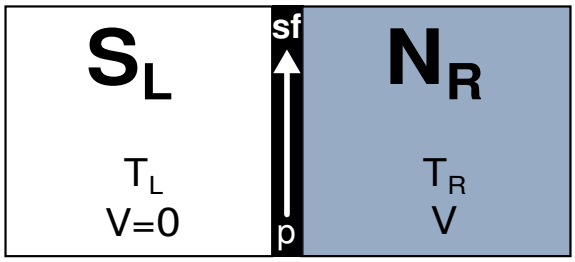

Figure 4.7: *Metallic and superconducting electrodes separated by a spin-filtering interlayer with filtering efficiency p.*

In oder to provide a quantitive description of the heat transport, we consider a system with a spin-filtering (or polarizing) barrier between a metallic and a superconducting electrode, as shown in Fig. 4.7. The current matrix in Eq. 3.15 can be generalized for the case of a spin-filtering barrier. Focusing on the tunneling limit, we can use the expression derived in [25],

$$\check{J} = \sum_n \frac{\tau_n}{2} \left[\check{\Gamma} \check{G}_S \check{\Gamma}, \check{G}_N \right]. \tag{4.6}$$

In the equation above, $\check{\Gamma}$ is a matrix that parametrices the effect of the spin-filter as follows:

$$\check{\Gamma} = t + u\hat{\tau}_3\hat{\sigma}_3, \tag{4.7}$$

where the parameters t and u are given by,

$$\left.\begin{array}{rcl} t & = & \sqrt{\frac{1+\sqrt{1-p^2}}{2}} \\ u & = & \sqrt{\frac{1-\sqrt{1-p^2}}{2}} \end{array}\right\}. \tag{4.8}$$

As tunnel limit is considered, only quasiparticle processes would contribute to the currents in Eq. 3.16. In order to consider Andreev reflection processes, we compute the anomalous GFs that is induced in the normal metal due to the proximity effect, *i.e.* the correction term that describes the penetration of the superconducting correlations in the normal metal, $\delta f^{R(A)}(x)$. In this case the GFs are space dependant:

$$\hat{G}_S^{R(A)} = g^{R(A)}\hat{\tau}_3 + if^{R(A)}\hat{\tau}_2,$$
$$\hat{G}_N^{R(A)} = \pm\hat{\tau}_3 + i\delta f^{R(A)}(x)\hat{\tau}_2$$
$$\hat{G}_S^K = \left(\hat{G}_L^R - \hat{G}_L^A\right) F_0,$$
$$\hat{G}_N^K = \hat{G}_N^R\left(F_+ + F_-\hat{\tau}_3\right) - \left(F_+ + F_-\hat{\tau}_3\right)\hat{G}_N^A.$$

We consider a quasi-1D situation and assume that δf only depends on the coordinate x. The $x = 0$ reference point is set at the N-S interface and x is assumed to be positive in the direction of the metallic electrode. The spacial dependance of $\delta f(x)$ can be obtained by solving the linearized Usadel equation 3.14,

$$\partial_{xx}\delta f^{R(A)} \pm \frac{2Ei}{D}\delta f^{R(A)} = 0, \tag{4.9}$$

which results into different solutions for the retarded and advanced Green's functions:

$$\delta f^R(x) = \hat{A}e^{(-1+i)\sqrt{E}x} \tag{4.10}$$
$$\delta f^A(x) = \begin{cases} \hat{B}^> e^{-(1+i)\sqrt{E}x} & E > 0 \\ \hat{B}^< e^{(1+i)\sqrt{E}x} & E < 0 \end{cases}. \tag{4.11}$$

Constants $\hat{A}$ and $\hat{B}^{\gtrless}$ may have non-trivial structure in the spin space. Using the boundary conditions for the current in the tunnel limit shown in Eq. 4.6, and identifying the current matrix with the one determined in Eq. 3.14, one gets the condition

$$\check{G}_N\partial_x\check{G}_N\Big|_{x=0} = \frac{\tau_n}{2}\left[\check{\Gamma}\check{G}_S\check{\Gamma}, \check{G}_N\right]_{x=0}, \tag{4.12}$$

that can be used to determine the values of $\hat{A}$ and $\hat{B}^{\gtrless}$. Writing the retarded and advanced components of the identity in the Eq. 4.12 and solving for the constants, one gets

$$A = \frac{\tau_n f^R\sqrt{1-p^2}}{\tau_n g^R + (1-i)\sqrt{E}},$$

$$B^{\gtrless} = \frac{\tau_n f^A\sqrt{1-p^2}}{\pm(1+i)\sqrt{E} - \tau_n g^A}.$$

As expected, as neither the spectrum of the metallic electrode nor the superconducting one depend on the spin, the proximity effect does not depend on it either. Adding the proximity effect correction to the GFs of the metallic electrode and calculating the current matrix using Eq. 4.6, charge and heat currents in Eq. 3.16 read,

$$I = \frac{e\sum_n \tau_n}{h}\int dE\left[-\frac{g^R-g^A}{2} + \frac{\sqrt{1-p^2}}{2}\frac{f^R+f^A}{2}(A+B^{\gtrless})\right]F_-, \tag{4.13}$$

$$Q = \frac{\sum_n \tau_n}{h}\int dE\; E\left[\frac{g^R-g^A}{2} - \frac{\sqrt{1-p^2}}{2}\frac{f^R-f^A}{2}(A-B^{\gtrless})\right](F_+ - F_0). \tag{4.14}$$

In the expressions above we have first and second order contributions to the currents with respect to the transmission coefficient, τ_n. First order contributions equal the current expressions in the tunneling limmit, so they can be rewritten as

$$1 \cdot \frac{g^R - g^A}{2} = \mathcal{N}_N(E)\cdot\mathcal{N}_S(E),$$

where $\mathcal{N}_{N/S}(E)$ stands for the density of states of the normal metal/superconductor. Second order contributions, i.e. those proportional to the constants A and $B^{\gtrless}$, describe effects related to higher order processes in tau (as the Andreev reflections). They can be suppressed with a perfect spin-filter ($p = 1$). In Fig. 4.4 we show that these currents contribute to the heat current at energies larger than the superconducting gap, whereas they contribute to the charge current at energies lower than Δ, i.e. Andreev reflections.

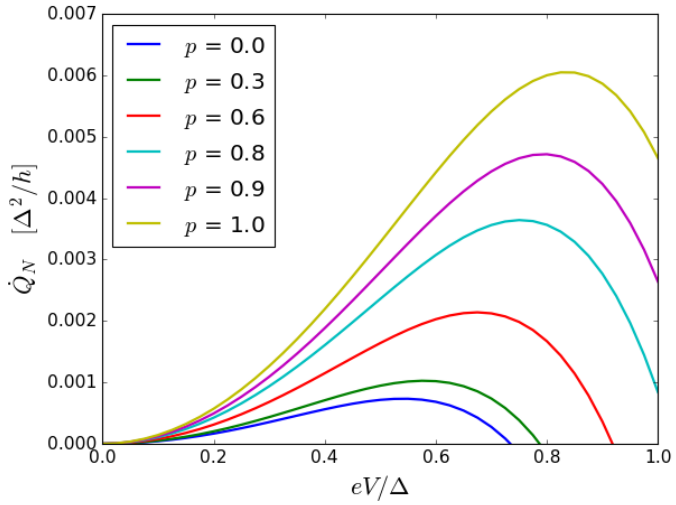

Figure 4.8: *Cooling power in the metallic electrode of a S-sf-N junction with $a\tau_n = 0.1$ and for different polarizations of the spin-filter at $T_N = T_S = 0.5T_C$. Increasing the efficiency of the spin-filter Andreev currents are turned off, which results into an enhancement in the cooling power.*

Cooling power in the metal is obtained by substracting the Joule heating (obtained from Eq. 4.13) to the heat current flowing out the metallic electrode (Eq. 4.14 with the opposite sign):

$$\dot{Q}_N = -(Q - IV). \tag{4.15}$$

Integrals in Eqs. 4.13-4.14 are computed numerically and the cooling power in the Eq. 4.15 is calculated and plotted in Fig. 4.8, where we have assumed that $T = 0.5T_C$. If we increase the efficiency of the spin-filtering barrier, p, the cooling power in the metallic electrode $\dot{Q}_N$ is largely enhanced. As it was discussed at the begining of the section, spin-filters turn off Andreev currents, decreasing dissipative currents in the metal, and, subsequently, increase its cooling power.

4.3 Heat Balance Equation and Calculation of the Electron Temperature.

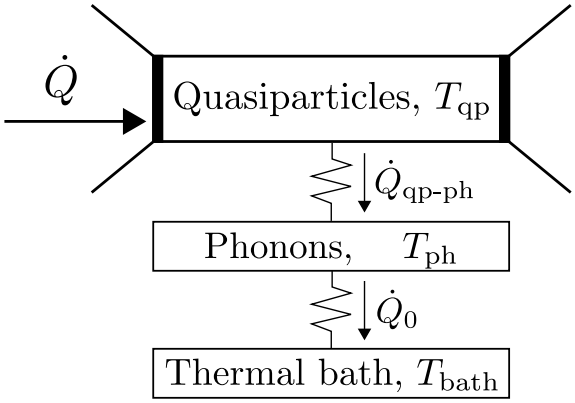

Figure 4.9: *Schematic picture of the whole system considered in the calculations. The heat flows between considered systems are represented by arrows.*

In previous sections we have mainly focused on the heat flow from one electronic system to another. However, these currents by their own do not give the accurate information about the final temperature of the quasiparticles. In order to calculate it, we must take into consideration not only the energy currents between the electronic systems that we have considered untill now, but also all possible heat transmission between the electrons and other constituents of the system, such a phonons.

Fig. 4.9 schematically shows a picture of the whole system. In the middle, we have the electronic system that we want to *refrigerate* (which refers to lowering the temperature, whereas *cooling* means keeping it at some desired value despite heating effects) forming an island between two electrodes at temperature $T_{\rm qp}$. $\dot{Q}$ is the *cooling power* that we have calculated in previous sections. Still, we now consider another system that coexists with the quasiparticles: the phonons. We assume that phonos are thermalised with the substrate and have a temperature T_{ph}. Via electron-phonon coupling there is a heat current between both systems $\dot{Q}_{\rm qp\text{-}ph}$. Finally, phonons also interact with a thermal bath at a temperature $T_{\rm bath}$ that acts as a reservoir. However, as the phonon system relaxation time is much faster than the one of the rest, we consider that $T_{\rm ph} = T_{\rm bath}$.

The final electronic temperature of the island is given by the quasiequilibrium situation in which all the heat currents flowing out from the system cancel,

$$\dot{Q} + \dot{Q}_{\text{qp-ph}} = 0. \tag{4.16}$$

The rate at which quasiparticles can transfer energy to the phonons, $\dot{Q}_{\text{qp-ph}}$, relies heavily on the spectral function of the system (i.e. whether it is a normal metal, a superconductor, if it is spin-split, etc.). In a normal metal it is given by [26]:

$$\dot{Q}_{\text{qp-ph}} = \Sigma\Omega k_B^5 \left(T_{\text{qp}}^5 - T_{\text{ph}}^5\right), \tag{4.17}$$

where Σ is a material dependent parameter that describes the coupling strength and Ω is the volume of the system. Values of Σ for some materials can be taken from [6].

Final temperature calculations in S-sf-N structures have been carried out in some recent works such as [8]. The process followed for obtaining these results is the next one:

1. Heat and charge currents are computed using Eq. 4.14 and Eq. 4.13 respectively for a guessed value of T_{qp}.

2. Coling power in the normal metal is obtained following Eq. 4.15. Results from the previous step are used in this one.

3. The heat current flowing from the quasiparticles to phonons is calculated using Eq. 4.17. In a normal metal, this is a simple expression. However, we will see that in a superconductor a double integral has to be numerically computed to obtain $\dot{Q}_{\text{qp-ph}}$.

4. The heat balance condiction is checked from Eq. 4.16. If this identity is not fulfilled, another value of T_{qp} is chosen and we go back to the first step.

Chapter 5

Effects of spin splitting on cooling in N-sf-S structures.

A superconductor responses to a magnetic field in two ways. On the one hand, the field creates circulating currents (Meissner effect), that try to expel the field from the bulk (diamagnetic response). By increasing the strength of the applied field, superconductivity is gradually reduced. This mechanism dominates in bulk samples or in thin films with the field applied perpendicular to the plane of the film.

On the other hand, the magnetic field may also try to align the spin of the electrons (Zeeman effect), resulting a paramagnetic response. This mechanism also leads to the suppression of superconductivit, and prevails with respect to the orbital one in two cases: superconducting films with thicknesses smaller than the London penetration length and magnetic fields applied parallel to the plane of the film. In this case, the magnetic field penetrates uniformly in the film and its critical value $H_{c\|}$ largely exceeds the critical value of a perpenciduclarly applied one $H_{c\perp}$[27, 28]. The paramagnetic effect in thin superconducting films leads to a Zeeman splitting of the density of states (DOS), equal to $2\mu_B|H| \equiv 2h$ as observed for the first time by Meservey *et al.* [29] in alluminium films.

An alternative way of creating a spin-split density of states in a superconductor is by means of the exchange field h induced by an adjacent ferromagnetic insulator (FI). This may lead to a large spin-splitting, even without an externally applied magnetic field. The first evidence of an exchange field induced in a superconductor via the proximity was measured in a thin Al film in contact with EuO film [30] and later on with EuS [31, 32].

The advantage of using a FI instead of an external magnetic field is that we avoid the depairing effects and all complications caused by the need of applying magnetic fields in superconducting devices. Moreover, FIs can also be used as spin-filtering barriers [33], which will play a crucial role in the structures discused in subsequent sections.

In this chapter we present novel results on the transport properties of hybrid

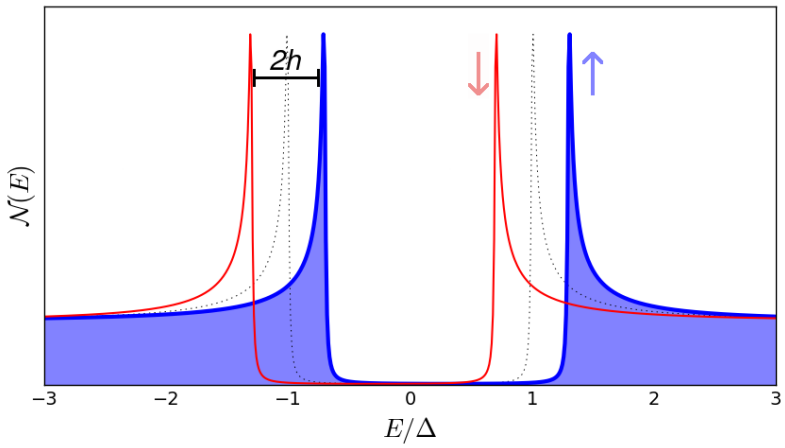

Figure 5.1: *Schematic picture of the effect that a spin-splitting h causes in spin-filtered transport. The blue (red) line represents the reduced DOS of spin up (down) quasiparticles. Assuming that the polarization of the spin-filter only allows quasiparticles with spin up to be transmitted (blue shaded DOS), the spin-splitting causes an effective bias in the superconductor, similar to the one an applied voltage causes, but without dissipation effects.*

structures that include spin-split superconductors, in particular SS-sf-N structures. The combination of spin-splitting and filtering effectively biases the DOS in the superconductor without any dissipative process (see Fig. 5.1 and its caption). In Sec. 5.1 we obtain the expression of the cooling power for both the spin-split superconductor and the normal metal in an island-like configuration, i.e. a normal (superconducting) island between two superconducting (normal) electrodes. On the one hand we show that it is possible to cool down a superconducting island with a spin-split DOS (section 5.2). On the other hand we prove that refrigeration of a normal island can be improved by using adjacent SS electrodes (sections 5.3.1 and 5.3.2).

5.1 The SS-sf-N Junction.

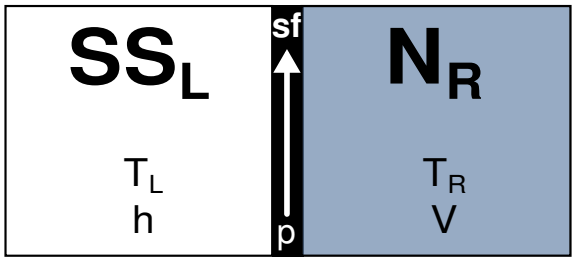

Figure 5.2: *Metallic and spin-split superconducting electrodes separated by a spin-filtering layer with filtering efficiency p.*

We consider a spin-filtering barrier with spin-filter efficiency p between a metallic and a superconducting electrode (see Fig. 5.2). The superconductor is spin-split

with an Zeeman field h parallel to the polarizacion direction of the spin-filter. The junction can be both temperature and potential biased. As we did in Sec. 4.2, we apply a space dependent correction term, $\delta f^{R(A)}(x)$, to the Green's functions to describe the proximity effect. In this case, the GFs present some structure in the spin space:

$$\begin{aligned}
\hat{G}_S^{R(A)} &= \left(\hat{g}_+^{R(A)} + \hat{g}_-^{R(A)}\hat{\sigma}_3\right)\hat{\tau}_3 + i\left(\hat{f}_+^{R(A)} + \hat{f}_-^{R(A)}\hat{\sigma}_3\right)\hat{\tau}_2, \\
\hat{G}_N^{R(A)} &= \pm\hat{\tau}_3 + i\delta f^{R(A)}(x)\hat{\tau}_2, \\
\hat{G}_S^{K} &= \left(\hat{G}_L^{R} - \hat{G}_L^{A}\right)F_0, \\
\hat{G}_N^{K} &= \hat{G}_N^{R}\left(F_+ + F_-\hat{\tau}_3\right) - \left(F_+ + F_-\hat{\tau}_3\right)\hat{G}_N^{A},
\end{aligned}$$

where

$$\begin{aligned}
g_\pm(E) &\equiv \tfrac{1}{2}[g(E+h) \pm g(E-h)], \\
f_\pm(E) &\equiv \tfrac{1}{2}[f(E+h) \pm f(E-h)].
\end{aligned}$$

The spacial dependance of $\delta f(x)$ can be obtained by solving the linearized Usadel equation (Eq. 4.9), which varies from the retarded to the advanced GFs:

$$\delta f^R(x) = \hat{A}e^{(-1+i)\sqrt{E}x} \tag{5.1}$$

$$\delta f^A(x) = \begin{cases} \hat{B}^{>}e^{-(1+i)\sqrt{E}x} & E > 0 \\ \hat{B}^{<}e^{(1+i)\sqrt{E}x} & E < 0 \end{cases}. \tag{5.2}$$

Constants $\hat{A}$ and $\hat{B}^{\gtrless}$ can be determined from the retarded and advanced components of the identity in Eq. 4.12. In this case, following the spin-dependance of the spectral functions of the system, the constants present some spin structure,

$$\begin{aligned}
\hat{A} &= A_1 + A_2\hat{\sigma}_3, \\
\hat{B}^{\lessgtr} &= B_1^{\lessgtr} + B_2^{\lessgtr}\hat{\sigma}_3,
\end{aligned}$$

where,

$$\begin{aligned}
A_1 &= \tfrac{\tau_n}{2}\frac{g_-^R A_2 - \sqrt{1-p^2}f_+^R}{X} & B_1^{\lessgtr} &= \tfrac{\tau_n}{2}\frac{g_-^A B_2^{\lessgtr} - \sqrt{1-p^2}f_+^A}{Y^{\lessgtr}} \\
A_2 &= -\sqrt{1-p^2}\tfrac{\tau_n}{2}\frac{Xf_-^R + \frac{\tau_n}{2}f_+^R g_-^R}{X^2 - (\frac{\tau_n}{2}g_-^R)^2} & B_2^{\lessgtr} &= \sqrt{1-p^2}\tfrac{\tau_n}{2}\frac{Y^{\lessgtr}f_-^A + \frac{\tau_n}{2}f_+^A g_-^A}{(Y^{\lessgtr})^2 - (\frac{\tau_n}{2}g_-^A)^2} \\
X &= (-1+i)\sqrt{E} - \tfrac{\tau_n}{2}g_+^R & Y^{\lessgtr} &= \mp(1+i)\sqrt{E} - \tfrac{\tau_n}{2}g_+^A
\end{aligned}.$$

The notation in the constant $\hat{B}^{\gtrless}$ means that

$$\hat{B}^{\gtrless} = \begin{cases} \hat{B}^{<} & \text{if} \quad E < 0 \\ \hat{B}^{>} & \text{if} \quad E > 0 \end{cases}.$$

As a perfect spin-filter turns down Andreev processes, when $p = 1$ is set, both constants are supressed, $\hat{A} = \hat{B}^{\gtrless} = 0$. We can now obtain the Keldysh component

of the current matrix in the tunnel limit from Eq. 4.6 and calculate the heat and charge currents by using Eq. 3.16 that read:

$$I = \frac{G_T}{4e}\int_{-\infty}^{\infty} dE\,\Big\{-(g_+^R - g_+^A)F_- + \frac{\sqrt{1-p^2}}{2}\times\Big[(A_1 + B_1^{\lessgtr})(f_+^R + f_+^A) + \\ + (A_2 + B_2^{\lessgtr})(f_-^R + f_-^A)\Big]F_- - p(g_-^R - g_-^A)(F_+ - F_0)\Big\}, \tag{5.3}$$

$$Q = \frac{G_T}{4e^2}\int_{-\infty}^{\infty} dE\;E\,\Big\{(g_+^R - g_+^A)(F_+ - F_0) - \frac{\sqrt{1-p^2}}{2}\times\Big[(A_1 - B_1^{\lessgtr})(f_+^R - f_+^A) + \\ + (A_2 - B_2^{\lessgtr})(f_-^R - f_-^A)\Big](F_+ - F_0) + p(g_-^R - g_-^A)F_-\Big\}, \tag{5.4}$$

where $G_T = \sum_n \tau_n G_0$ is the conductance of the junction. In these expressions we can distinguish the first order quasiparticle contributions to the currents, described by standard GFs g, from the the second order Andreev-like ones, which are proportional to the constants $A_{1,2}$ $B_{1,2}^{\lessgtr}$ and can contribute at energyes larger or lower than the superconducting gap (see Fig. 4.4).

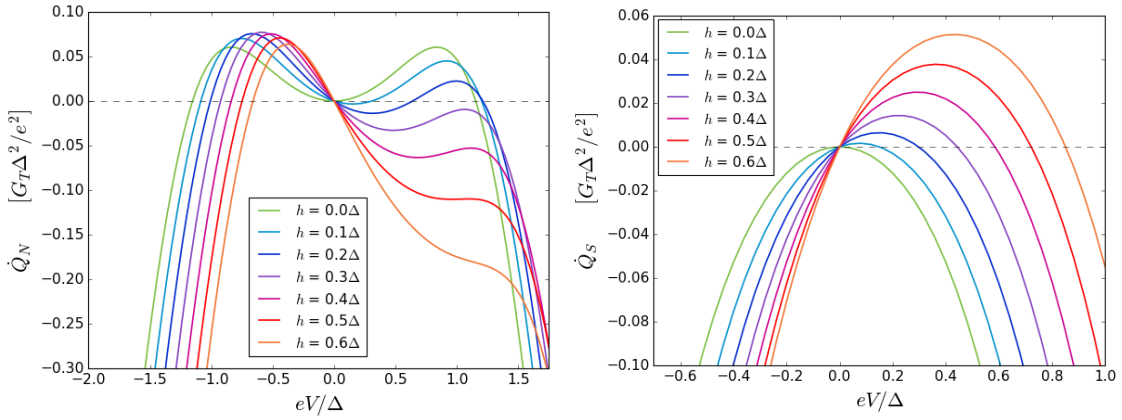

(a) **(b)**

Figure 5.3: *Cooling power in* ***(a)*** *the normal metal and* ***(b)*** *the spin-split superconductor in a SS-sf-N junction in terms of eV and for different values of the splitting field h. Perfect spin-filter, $p = 1$, and $T_S = T_N = 0.5T_C$, where T_C is the transition temperature of the superconducting phase, is assumed.*

From the expressions of the heat and charge currents above, the cooling power in both the metallic and the superconducting electrodes, $\dot{Q}_{S/N}$, can be computed as follows:

$$\dot{Q}_{S/N} = \pm(Q - IV_{S/N}), \tag{5.5}$$

where $V_{S/N}$ is the voltage applied to the electrode, i.e. always zero in the superconductor and V in the normal metal. In Fig. 5.3 we numerically calculate the charge and heat currents in Eqs. 5.3 and 5.4 respectively and use Eq. 5.5 to obtain the

cooling power in both the metallic and the superconducting electrodes. These calculations have been done for $T_N = T_S = 0.5T_C$, where T_C is the critical temperature of the superconducting phase and supposing a perfect spin-filtering, $p = 1$.

In the case of the metallic electrode, the maximum value of the cooling power is slightly enhanced, being as maximum at values of $h \approx 0.3\Delta$. However, the most important impact of the spin-splitting in the cooling power is the shift of its maximum value to lower values of V. This leads to lower dissipation effects, heating less the enviroment and hence, improving the refrigeration of a metallic island when non-infinite superconducting electrodes are considered.

The change in the cooling power of the superconducting electrode when it is spin-split has much more interest. Contrary to the structures that we have studied in chapter 4, in Fig. 5.3 a possibility to refrigerate a superconducting island via two metallic electrodes is observed.

In subsequent sections we study the refrigeration of the normal metal and the superconductor for different values of the Zeeman field h in island-like structures.

5.2 Refrigeration of a Spin-Split Superconductor (N-sf-SS-sf-N).

In this section we study the refrigeration of a spin-split superconducting island between two infinite-metallic electrodes. Both junctions are assumed to be equal and very resistive, such that a potential drop V through the whole nanostructure corresponds to a drop of $V/2$ in each of the junctions. Polarization directions of the spin-filters of the junctions are opposited to the other to maximize the total cooling power in the island. In this configuration, the quasiequilibrium condition for the heat currents flowing out from the island in Eq. 4.16 reads,

$$2\dot{Q}_S + \dot{Q}_{\text{qp-ph}} = 0, \tag{5.6}$$

where $\dot{Q}_S$ is the one shown in Eq. 5.5 and $\dot{Q}_{\text{qp-ph}}$ is the heat current flowing from the electronic systems to the phonons in the superconductor. In a spin-split superconductor this current is calculated as follows [34]:

$$\begin{aligned}\dot{Q}_{\text{qp-ph}} = &-\frac{\Sigma\Omega}{96\zeta(5)k_B^5}\int_{-\infty}^{\infty} dE\; E\int_{-\infty}^{\infty} d\omega\; \omega^2\; sgn(\omega) L_{E,E+\omega}\Bigg\{\coth\left(\frac{\omega}{2k_BT_{ph}}\right)\times \\ &\left[\tanh\left(\frac{E}{2k_BT_{qp}}\right)\tanh\left(\frac{E+\omega}{2k_BT_{qp}}\right)\right] - \tanh\left(\frac{E}{2k_BT_{qp}}\right)\tanh\left(\frac{E+\omega}{2k_BT_{qp}}\right) + 1\Bigg\},\end{aligned} \tag{5.7}$$

where Σ is a constant describing the coupling strength, Ω stands for the sample volume, $\zeta(x)$ is the Riemman's function, h stands for the Zeeman splitting and $L_{E,E'}$ is the kernel of the integral, that reads:

$$L_{E,E'} = \frac{1}{2}\sum_{\sigma=\pm} N_S(E_\sigma)N_S(E'_\sigma)\left[1 - \frac{\Delta(T_{qp})}{E_\sigma E'_\sigma}\right] \tag{5.8}$$

In the normal case, $\Delta = 0$, and absence of spin-splitting, $h = 0$, the collision integral in Eq. 5.7 can be analitically solved, resulting into Eq. 4.17.

In order to simplify the notation when solving Eq. 5.10, we group all the parameters in a dimensionless one, which we defined as

$$\tilde{\Sigma} \equiv \frac{\Sigma\Omega\Delta^3 e^2}{G_T k_B^5}. \tag{5.9}$$

Values of the coupling parameter, Σ, can be taken from [6]. To get a clear picture of which are the involved magnitudes, taking values of the parameters for an alluminium $\Omega \sim \mu m^3$ volume island, a value of $\tilde{\Sigma} = 300$ corresponds to a junction with a resistance of $R_T \sim 1k\Omega$.

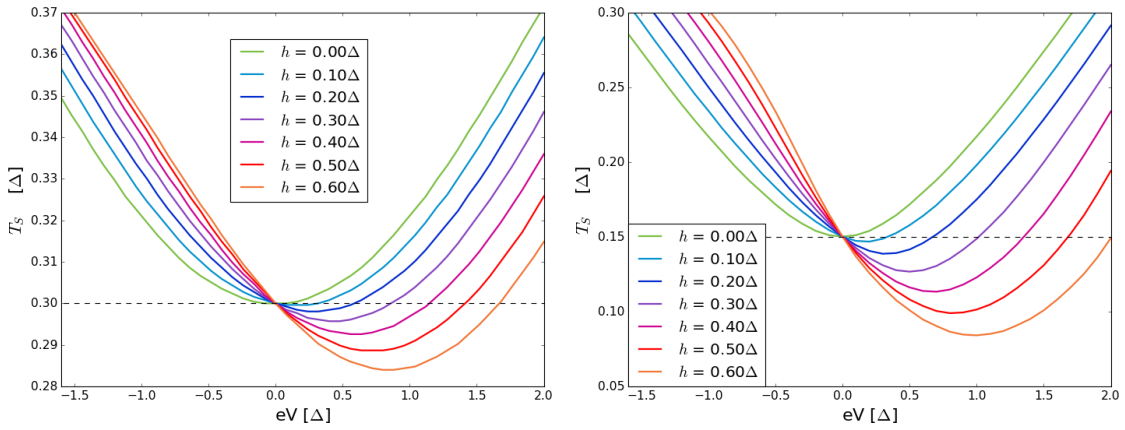

Figure 5.4: *Final temperature of quasiequilibrium of the superconducting island in terms of the voltage drop in the nanostructure for* $\tilde{\Sigma} = 300$ *and* ***(a)*** $T_{ph} = 0.3\Delta$ *and* ***(b)*** $T_{ph} = 0.15\Delta$.

In Fig. 5.4 the final temperature of the quasiparticles in the spin-split superconducting island is shown in terms of the applied voltage in the whole nanostructure, for $\tilde{\Sigma} = 300$ and for different splitting amplitudes. To do that we numerically calculate charge and heat currents using Eqs. 5.3 and 5.4 respectively and inserted them in Eq. 5.5 to obtain the cooling power. After that, we numerically compute the heat current from the quasiparticles to the phononic system in a spin-split superconductor (see Eq. 5.7) and check the heat balance condition in Eq. 5.10. This is repeated untill we find the quasiequilibrium electronic temperature $T_{\rm qp}$. Infinite normal electrodes have been assumed, so the value of the quasiparticle-phonon collision integral (Eq. 4.17) is so high that the temperature of the quasiparticles in those will be equal to the phonon's temperature, $T_N = T_{\rm ph}$. Phonons, on the other hand, are in equilibrium with the thermal bath and hence present the same temperature in the whole structure.

In the absence of spin-spliting, the superconducting island cannot be refrigerated, while an increase of h leads to an enhancement in its refrigeration. Moreover, this refrigerating efficiency depends much on the reservoir's (metallic infinite electrodes) temperature. If the superconductor is suposed to be alluminium ($\Delta = 180\mu eV$), Fig. 5.4b would suggest, for a $h = 0.5\Delta$ splitting amplitude, a decrease in the temperature of the quasiparticles from about $300mK$ to $200mK$. In subsequent sections we see that this refrigeration is comparable to the one observed in a metallic island with the same parameter $\tilde{\Sigma} = 300$ (see Fig. 5.5).

5.3 Normal Metal Refrigeration (SS-sf-N-sf-SS).

In this section we study the refrigeration of a metallic island between two spin-split superconducting electrodes. Polarization directions of the spin-filters of the junctions are opposited to the other to maximize the total cooling power in the island. The structure is suposed to be perfectly symmetric, so the potential drop in each junction, $V/2$, is the half of the total potential drop in the nanostructure V. We consider two different situations: *(Sec. 5.3.1)* infinite superconducting electrodes and *(Sec. 5.3.2)* superconducting electrodes with finite volume.

5.3.1 Infinite Electrodes

As the spin-split superconducting electrodes' volume is suposed to be infinite (i.e. many orders of magnitude larger than the metallic island's), $\tilde{\Sigma}_S \to \infty$. Therefore, the temperature of the quasiparticles will be the same as the phononic one, $T_S = T_{\mathrm{qp}}$, which is constant due to the thermal bath. In this configuration, the quasiequilibrium condition for the heat currents flowing out from the island in Eq.

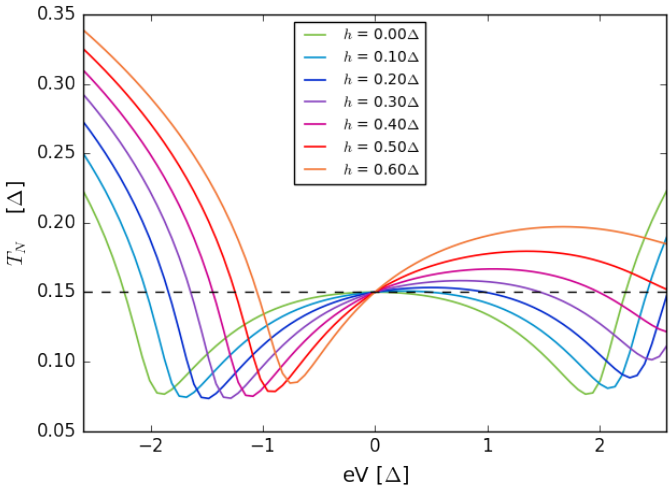

Figure 5.5: *Final temperature of the metallic island in terms of the potential drop in the nanostructure for different values of h and a qp-ph coupling parameter* $\tilde{\Sigma}_N = 300$.

4.16 reads:

$$2\dot{Q}_N + \dot{Q}_{\text{qp-ph}} = 0, \tag{5.10}$$

where $\dot{Q}_N$ is described in Eq. 5.5 and $\dot{Q}_{\text{qp-ph}}$ is the heat current flowing from the electronic systems to the phonons in the normal metal, given by Eq. 4.17.

In Fig. 5.5 the final temperature of the quasiparticles in the metallic island is shown for different values of h and in terms of the applied bias voltage to the nanostructure. In the metallic island a parameter of $\tilde{\Sigma}_N = 300$ is chosen.

When the spin-split superconducting electrodes are assumed to be infinite, the enhancement in the refrigeration of metallic island with the splitting amplitude h is negligible. The main effect of the splitting in the electrodes is the shift of the minimum final temperature to lower values of bias voltage, i.e. to regions with lower dissipation.

5.3.2 Finite Electrodes

As we have shown in the previous section, spin-splitting the superconducting electrodes moves the maximum in refrigeration of the island to regions with lower Joule heating, thus, decreasing the heating of the enviroment. We consider now a metallic island connected to two finite spin-split superconducting electrodes through a spin-filter. We choose a limit case where the coupling parameters are equal in the island and the electrodes, $\tilde{\Sigma}_S = \tilde{\Sigma}_S = 300$. This is not quite a realistic setup, as in experiments the electrodes are much larger than the islands, but it helps to understand the behaviour of the refrigeration of the island when the *electrodes* connected to it are not reservoirs.

In this case, the final temperatures of qusiparticles in both, the normal metal

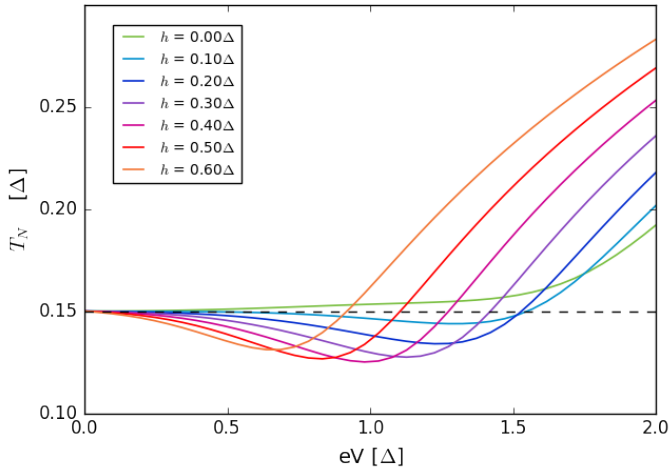

Figure 5.6: *Final temperature of the metallic island in terms of the potential drop in the nanostructure for different values of h and qp-ph coupling parameters* $\tilde{\Sigma}_S = \tilde{\Sigma}_N = 300$.

and the spin-split superconductor, must be computed. We have now an equation system formed by two heat balance equations of Eq. 4.16 to obtain T_S and T_N,

$$\begin{cases} 2\dot{Q}_N + \dot{Q}^N_{\text{qp-ph}} = 0 \\ \dot{Q}_S + \dot{Q}^S_{\text{qp-ph}} = 0 \end{cases} , \tag{5.11}$$

where $\dot{Q}_{n/s}$ are numerically calculated following Eq. 5.5 nad $\dot{Q}^N_{\text{qp-ph}}$ and $\dot{Q}^N_{\text{qp-ph}}$ are obtained from Eq. 4.17 and Eq. 5.7 respectively.

In Fig. 5.6 the final temperature of the quasiparticles in the metallic island is shown for different values of h and in terms of the applied voltage. We observe that, when superconducting electrodes are finite, one can enhance the refrigeration of the N island by spin-splitting the superconductors. This enhancement is due to the lower dissipative currents flowing at the maximum of the cooling power, which decreases the heating of the electrodes and hence, increases the cooling power in the metal $\dot{Q}_N(V, T_N, T_S)$.

Chapter 6

Summary.

The present Master's Thesis deals with the study of the electronic cooling of some sections of junctions composed by normal metals and/or superconductors. Discussed thermoelectric effects are originated from the coupling between charge and current. We have described some novel results in normal metal - spin filter - spin-split superconductor structures (N-sf-SS). In particular, the spin-splitting opens the possibility of cooling the superconductor and enhances the refrigeration of the normal metal.

In chapters 2 and 3, we present the main theoretical tool used in this work, *i.e.* the quasiclassical Keldysh Green function formalism, and discussed its benefits over the more used Landauer-Büttiker formalism. In addition, we also solve some examples with a pedagogical purpose.

In chapter 4, we introduce the concept of *cooling power* by means of the widely studied N-S structure and how it can be enhanced placing a spin-filter between the electrodes to shut down the Andreev currents. We also present the collision integral that describes quasiparticle-phonon coupling in normal metals and let us obtain its final quasiequilibrium temperatures.

The chapter 5 summarizes the novel results obtained from the study of the N-sf-SS system. The combination of the spin-splitting and the spin-filter effectively biases the spectrum of the superconductor without any dissipative effect (i.e. without changing the Fermi level). For each spin species the electron-hole symmetry is broken.

The non-dissipative biasing technique has two effects in the cooling power of the parts of the system. On the one hand, we can refrigerate the spin-split superconductor extracting hot carriers to the metal. This is impossible in other configurations, as the superconductor is the element acting as an energy filter due to its electronic gap. Furthermore, the drops in temperature obtained in the superconductor for splitting fields of $h \approx 0.5\Delta$ are comparable to those of the metal in N-sf-S structures. This new refrigeration possibility, in addition to its fundamental utility, might result in some interesting applications for quantum technologies.

On the other hand, the additional bias caused by the exchange field h, shifts the maximum cooling power in the metal to lower values of applied voltage V, which implies lower ohmic dissipation rates. As a result, the heating of the adjacent superconducting sample is reduced, hence enhancing the refrigeration of the normal metal. The more similar the volumes of the spin-split superconducting and metallic samples are, the more remarkable is the improvement.

As further research we propose the study of the cooling power on spin-split superconductor - spin-filter - superconductor (SS-sf-S') structures. Some preliminary calculations suggest that these structures may improve it. The maximum value of the cooling power is present when the coherent peaks at the gap edges of both superconductors are aligned. The cooling power around those voltages shows a peak with a width and height that strongly depends on the damping parameter. Further studies are being done in this direction.

Bibliography

[1] H Kamerlingh Onnes. The resistance of pure mercury at helium temperatures. *Commun. Phys. Lab. Univ. Leiden*, 12(120):1, 1911.

[2] GE Blonder, M Tinkham, and TM Klapwijk. Transition from metallic to tunneling regimes in superconducting microconstrictions: Excess current, charge imbalance, and supercurrent conversion. *Physical Review B*, 25(7):4515, 1982.

[3] TM Klapwijk, GE Blonder, and M Tinkham. Explanation of subharmonic energy gap structure in superconducting contacts. *Physica B+ C*, 109:1657–1664, 1982.

[4] RC Jaklevic, John Lambe, AH Silver, and JE Mercereau. Quantum interference effects in josephson tunneling. *Physical Review Letters*, 12(7):159, 1964.

[5] MM Leivo, JP Pekola, and DV Averin. Efficient peltier refrigeration by a pair of normal metal/insulator/superconductor junctions. *Applied physics letters*, 68(14):1996–1998, 1996.

[6] Francesco Giazotto, Tero T Heikkilä, Arttu Luukanen, Alexander M Savin, and Jukka P Pekola. Opportunities for mesoscopics in thermometry and refrigeration: Physics and applications. *Reviews of Modern Physics*, 78(1):217, 2006.

[7] HQ Nguyen, JT Peltonen, Matthias Meschke, and JP Pekola. Cascade electronic refrigerator using superconducting tunnel junctions. *Physical Review Applied*, 6(5):054011, 2016.

[8] A Ozaeta, AS Vasenko, FWJ Hekking, and FS Bergeret. Electron cooling in diffusive normal metal–superconductor tunnel junctions with a spin-valve ferromagnetic interlayer. *Physical Review B*, 85(17):174518, 2012.

[9] Mikel Rouco, Tero T Heikkilä, and FS Bergeret. Electron refrigeration in nanostructures with spin-split superconductors. *in preparation*, 2017.

[10] R. Landauer. Spatial variation of currents and fields due to localized scatterers in metallic conduction. *IBM Journal of Research and Development*, 1(3):223–231, July 1957.

[11] Rolf Landauer. Electrical resistance of disordered one-dimensional lattices. *Philosophical Magazine*, 21(172):863–867, 1970.

[12] M. Büttiker, Y. Imry, R. Landauer, and S. Pinhas. Generalized many-channel conductance formula with application to small rings. *Phys. Rev. B*, 31:6207–6215, May 1985.

[13] B. J. van Wees, H. van Houten, C. W. J. Beenakker, J. G. Williamson, L. P. Kouwenhoven, D. van der Marel, and C. T. Foxon. Quantized conductance of point contacts in a two-dimensional electron gas. *Phys. Rev. Lett.*, 60:848–850, Feb 1988.

[14] JI Pascual, J Méndez, J Gómez-Herrero, AM Baró, N Garcia, and Vu Thien Binh. Quantum contact in gold nanostructures by scanning tunneling microscopy. *Physical review letters*, 71(12):1852, 1993.

[15] A. A. Abrikosov. *Fundamentals of the Theory of Metals*. North-Holland Amsterdam, 1988.

[16] Alexandre M Zagoskin. *Quantum theory of many-body systems*. Springer, 1998.

[17] Alekseĭ Alekseevich Abrikosov, Lev Petrovich Gorkov, and Igor Ekhielevich Dzyaloshinski. *Methods of quantum field theory in statistical physics*. Dover, 1963.

[18] Yaroslav M. Blanter Yuli V. Nazarov. *Quantum transport: introduction to nanoscience*. Cambridge University Press, 1 edition, 2009.

[19] S Kolenda, MJ Wolf, and D Beckmann. Observation of thermoelectric currents in high-field superconductor-ferromagnet tunnel junctions. *Physical review letters*, 116(9):097001, 2016.

[20] M Nahum, Travis M Eiles, and John M Martinis. Electronic microrefrigerator based on a normal-insulator-superconductor tunnel junction. *Applied Physics Letters*, 65(24):3123–3125, 1994.

[21] AM Clark, NA Miller, A Williams, ST Ruggiero, GC Hilton, LR Vale, JA Beall, KD Irwin, and JN Ullom. Cooling of bulk material by electron-tunneling refrigerators. *Applied Physics Letters*, 86(17):173508, 2005.

[22] Peter J Lowell, Galen C O'Neil, Jason M Underwood, and Joel N Ullom. Macroscale refrigeration by nanoscale electron transport. *Applied Physics Letters*, 102(8):082601, 2013.

[23] Juha T Muhonen, Matthias Meschke, and Jukka P Pekola. Micrometre-scale refrigerators. *Reports on Progress in Physics*, 75(4):046501, 2012.

[24] JS Moodera, R Meservey, and X Hao. Variation of the electron-spin polarization in euse tunnel junctions from zero to near 100% in a magnetic field. *Physical review letters*, 70(6):853, 1993.

[25] FS Bergeret, Alvise Verso, and Anatoly F Volkov. Electronic transport through ferromagnetic and superconducting junctions with spin-filter tunneling barriers. *Physical Review B*, 86(21):214516, 2012.

[26] FC Wellstood, C Urbina, and John Clarke. Hot-electron effects in metals. *Physical Review B*, 49(9):5942, 1994.

[27] R Meservey and PM Tedrow. Properties of very thin aluminum films. *Journal of Applied Physics*, 42(1):51–53, 1971.

[28] Michael Tinkham. *Introduction to superconductivity*. Courier Corporation, 1996.

[29] R Meservey, PM Tedrow, and Peter Fulde. Magnetic field splitting of the quasiparticle states in superconducting aluminum films. *Physical Review Letters*, 25(18):1270, 1970.

[30] PM Tedrow, JE Tkaczyk, and A Kumar. Spin-polarized electron tunneling study of an artificially layered superconductor with internal magnetic field: Euo-al. *Physical review letters*, 56(16):1746, 1986.

[31] X Hao, JS Moodera, and R Meservey. Spin-filter effect of ferromagnetic europium sulfide tunnel barriers. *Physical Review B*, 42(13):8235, 1990.

[32] MJ Wolf, C Sürgers, G Fischer, and D Beckmann. Spin-polarized quasiparticle transport in exchange-split superconducting aluminum on europium sulfide. *Physical Review B*, 90(14):144509, 2014.

[33] Jagadeesh S Moodera, Tiffany S Santos, and Taro Nagahama. The phenomena of spin-filter tunnelling. *Journal of Physics: Condensed Matter*, 19(16):165202, 2007.

[34] Nikolai B Kopnin. *Theory of nonequilibrium superconductivity*, volume 110. Oxford University Press, 2001.